Effects of S100A8/S100A9 (calprotectin) on human respiratory mucosal epithelium and its regulatory mechanism

Sang Hyeon Ahn
Department of Medicine
The Graduate School, Yonsei University

Effects of S100A8/S100A9 (calprotectin) on human respiratory mucosal epithelium and its regulatory mechanism

Sang Hyeon Ahn
Department of Medicine
The Graduate School, Yonsei University

Effects of S100A8/S100A9 (calprotectin) on human respiratory mucosal epithelium and its regulatory mechanism

Directed by Professor Chang-Hoon Kim

The Doctoral Dissertation
submitted to the Department of Medicine,
the Graduate School of Yonsei University
in partial fulfillment of the requirements for the degree of
Doctor of Philosophy in Medical Science

Sang Hyeon Ahn

December 2022

This certifies that the Doctoral Dissertation of Sang Hyeon Ahn is approved.

Thesis Supervisor: Chang-Hoon Kim

Thesis Committee Member#1: Sang Sun Yoon

Thesis Committee Member#2: Jin Kook Kim

Thesis Committee Member#3: Hyoung-Pyo Kim

Thesis Committee Member#4: Hyung-Ju Cho

The Graduate School

Yonsei University

December 2022

ACKNOWLEDGMENTS

There were a lot of big and small events in my thirties. During that time, I got married and started a family. In addition, I became an otorhinolaryngologist and majored in the subspecialty of rhinology. Most of all, I started and finally finished my Ph.D. in medicine, and I would like to thank my acquaintances who helped me achieve this.

First of all, I would like to thank Professor Chang-Hoon Kim, who was a mentor for the master's and doctoral degree programs and taught me rhinology. When I first told him I wished to learn rhinology, he told me not to give up and to experiment until the very end, which gave me hope that I could finish my course. In addition, a piece of advice from Professor Joo-Heon Yoon—to do everything happily—became a point of wisdom in my life. I would also like to express my gratitude to Professor Hyung-Ju Cho, who supported me both academically and mentally during the course of the degree. Furthermore, I would like to express my gratitude to Professor Kyung-Su Kim for their unwavering encouragement as it helped me a lot in completing the Ph.D. program.

The members of the committee offered me a lot of advice from the beginning to the end of the doctoral degree program. I would like to thank Professors Sang Sun Yoon and Hyung-Pyo Kim, who gave me encouragement and advice so that I could finish my degree safely. I would also like to thank Professor Jin Kook Kim, who gave me confidence in the midst of setbacks.

In the laboratory, there were many persons who gave me technical advice on experimental and scientific thinking in biology. First of all, I would like to thank Sang-Nam Lee, Ph.D. and Hong-Kyung Kim, Ph.D. for their encouragement and assistance in designing the experiment and analyzing the results. I am also grateful to the many researchers at The Airway Mucus Institute who actively helped with the experiment. I would also like to express my deepest gratitude to Sang Chul Park, Eun Jung Lee, and Min-Seok Rha, who helped me interpret the experiment and derive good results as senior doctors of medicine and of philosophy. In addition, Kye Won Kwon, M.D., Ph D. and

Sugyeong Jang, pathologists at Bundang Jesaeng Hospital, contributed greatly to the analysis of human tissues. Furthermore, I would like to thank my friends outside my laboratory, Daehyun Park, Joseph Park, and Changhee Park, who listened to my concerns and difficulties during the degree course and gave me advice as senior doctors of philosophy.

Above all, I am most grateful to Eun Young Lee, M.D., my life companion and my wife, who generously gave me practical advice and objective criticism on medicine and academics. Thank you to my precious son, Yun Ho Ahn, and my daughter, Ye Eun Ahn, for always being by my side and supporting me. I would also like to thank my father, Gi Eob Ahn, and my mother, Hyun Ho Choi, who always supported and encouraged me until the end to finish my degree, and I am grateful to my younger sister Hyeon and her family—Sang Ryul Ahn, Ji Hun, Jae Hee, and Jun Ho. I would also like to thank my father-in-law and mother-in-law for helping me focus on my work and studies. Furthermore, I would like to express my sincere gratitude to my uncle Wan Ho Choi, who rejoiced in good things coming together, listened to my concerns during difficult times, and suggested solutions to problems.

Lastly, I am most grateful to myself for not giving up and for enduring all of these processes over the past 10 years. Getting a Ph.D. was a road that no one had taken before and was not an easy process to navigate. However, when I analogize my experience with a long tunnel I went through and looked back, it was a meaningful time for me to become more mature. In addition, the times when I could not sleep, was troubled, and solved problems were fun times and precious memories that showed that challenge in my life are worth taking.

Sang Hyeon Ahn

Yonsei University, College of Medicine

December, 2022

TABLE OF CONTENTS

CHAPTER II.

LIST OF FIGURES

LIST OF TABLES

ABSTRACT

Effects of S100A8/S100A9 (calprotectin) on human respiratory mucosal epithelium and its regulatory mechanism

Sang Hyeon Ahn

Department of Medicine
The Graduate School, Yonsei University

(Directed by Professor Chang-Hoon Kim)

Inflammation is a host's defense mechanism against external stimulants, and the immune response by the first frontline barrier epithelium and inflammatory cells is complexly generated. Chronic rhinosinusitis (CRS) is a chronic inflammatory disease that occurs in the paranasal sinuses. A number of substances are involved in the immune response of CRS, and various pathophysiological mechanisms have been suggested. In particular, calprotectin as a damage-associated molecular pattern is a heterodimer complex of S100A8 and S100A9 and performs various functions in epithelial and inflammatory cells. In addition, although S100A8 and S100A9 are known to have strong pro-inflammatory effects, studies on their effects on the human nasal epithelial (HNE) cells and pathogenesis of CRS are rare. Therefore, this study aimed to investigate the effects of S100A8, S100A9, and calprotectin on human nasal epithelium, CRS, and regulatory mechanisms.

Chapter I explores the conditions under which S100A8 and S100A9 are elevated in the upper airway nasal epithelium and investigates the roles of S100A8 and S100A9 in HNE cells. S100A8 and S100A9 increased when pro-inflammatory cytokines, such as TNF-α

and IL-1β, were treated. They were inhibited by anti-inflammatory cytokines, such as IL-4 and IL-13. In addition, they were overexpressed in the squamous epithelium, not in normal tissues, through immunohistochemical findings of CRS tissues. In order to check whether S100A8 and S100A9 affect squamous metaplasia, recombinant S100A8, S100A9, and calprotectin were applied to HNE cells. Matrix metalloproteinase 9 (MMP9), a marker for tissue remodeling, and Involucrin, a marker for squamous metaplasia, were then used to confirm the optimal experimental conditions. Furthermore, the effects of S100A8, S100A9, and calprotectin on HNE cells were investigated through bulk RNA sequencing analysis. It was particularly confirmed that S100A9 induces squamous metaplasia by being involved in retinoic acid metabolism, which is important for HNE cells differentiation.

In Chapter II, the role of calprotectin, known as an antimicrobial peptide, on eosinophils and eosinophil extracellular traps (EETs) in the pathophysiology of CRS is investigated. Previously, calprotectin was known to be predominantly expressed in neutrophils and be mainly involved in neutrophil extracellular traps (NETs). However, CRS with nasal polyps (CRSwNP) insufficiently explained the presence of only calprotectin and neutrophil because eosinophils were known to be important type 2 inflammation cells in disease development. Therefore, the purpose of this study was to investigate the relationship between calprotectin and eosinophil and between calprotectin and EETs. To prove this hypothesis, using eosinophilic CRS mouse and human tissues, major basic protein (MPB) and myeloperoxidase (MPO), which are markers specific to eosinophils and neutrophils, respectively, were subjected to simultaneous immunofluorescence with calprotectin. As a result, calprotectin-positive cells were co-localized with MBP-positive cells, and calprotectin was involved in EETs as well as NETs. In addition, calprotectin-positive cells in the tissue showed a positive correlation with tissue and blood eosinophils. Additionally, calprotectin showed a correlation with olfactory dysfunction, with the Lund-Mackay CT score indicating the severity of CRS and the use of JECREC scores. Through this, it was demonstrated that the expression of

calprotectin in CRS tissue can be a biomarker indicating disease severity.

Summarizing these two studies, increased S100A8 and S1000A9 due to inflammation in HNE cells induces tissue remodeling, such as squamous metaplasia through the modulation of retinoic acid metabolism. In addition, calprotectin is secreted by neutrophils and eosinophils and has an important role in the innate immune response of CRSwNP, owing to its involvement in EETs. In conclusion, S100A8, S100A9, and calprotectin expressed in epithelial and inflammatory cells reflect the disease severity of patients with CRS.

Key words : S100A8, S100A9, leukocyte L1 antigen complex, nasal mucosa, airway remodeling, sinusitis, nasal polyps, anti-microbial peptides, eosinophils, extracellular traps

Effects of S100A8/S100A9 (calprotectin) on human respiratory mucosal epithelium and its regulatory mechanism

Sang Hyeon Ahn

Department of Medicine
The Graduate School, Yonsei University

(Directed by Professor Chang-Hoon Kim)

Chapter I.

S100A8 and S100A9 induce tissue remodeling via modulation of retinoic acid metabolism in human nasal epithelium.

I. INTRODUCTION

The human nasal epithelium of the upper respiratory tract is the first frontline site to be directly exposed to inhaled environmental stressors, such as pathogens, allergens, or air pollutants[1,2]. The airway epithelium is composed of three layers (mucus layer, epithelium, and basement membrane) and acts as a chemical and physical barrier against external stimuli[3]. The human nasal epithelial (HNE) cells, which are composed of pseudostratified columnar epithelial cells, goblet cells, and basal cells, play an important switchboard role in recognizing pathogens through pattern recognition receptors (PRRs) and regulating immune responses by secreting antimicrobial agents and danger-associated molecular patterns (DAMPs)[3,4].

Inflammation in nasal epithelium is a defense response of the immune system to dangerous stimulus, such as pathogens, damaged cells, and toxic compounds from the external environment[5]. Various types of secreted polypeptides, known as cytokines and DAMPs, are secreted during the inflammatory response, causing the removal of external harmful stimuli or adapting to stimuli through tissue healing and repair[6,7]. Tissue remodeling as a result of tissue repair occurs as an adaptive response to stress when external stimulation continues repeatedly for a long duration[8]. Therefore, tissue remodeling is particularly well-observed in chronic diseases. In particular, chronic rhinosinusitis (CRS) caused by chronic inflammation in the nasal cavity can also be observed to change normal nasal epithelium into various morphologies[9]. Tissue remodeling in CRS includes subepithelial fibrosis, goblet cell hyperplasia, basement membrane thickening, and squamous metaplasia[10].

Squamous metaplasia, one type of tissue remodeling, is defined as a change from a ciliated pseudostratified columnar epithelium, a typical nasal mucosal structure, to a non-keratinized squamous epithelium due to chronic inflammation[11]. Squamous metaplasia is the most severe and irreversible change in epithelial remodeling and is an adaptive change that occurs because it is more resistant than are other tissues to external stimuli[12]. In previous reports, squamous metaplasia can be found in 6–18% of CRS tissue

and in 23–25% of nasal polyps[11,13,14]. In addition, squamous metaplasia in CRS tissue is related to the severity of chronic inflammation[11] or CRS severity[15].

S100A8 and S100A9, also known DAMPs, have potent pro-inflammatory activity[16,17]. S100A8 and S100A9 are known to be secreted mainly from neutrophils but are also known to be secreted from non-keratinizing squamous epithelial cells under inflammation[18]. In particular, in skin, S100A8 and S100A9 are known to play a major role in the formation of the squamous epithelial barrier by regulating keratinocyte proliferation and differentiation[19]. On the other hand, it has been reported that S100A8 and S100A9 affect epithelial barrier function in the tissues of patients with CRS[20,21]. In addition, S100A8 and S100A9 were found to be involved in inflammatory reactions and tissue remodeling together with their complex calprotectin, known as an antimicrobial peptide[22,23]. However, the function of S100A8 and S100A9 in tissue remodeling, such as squamous metaplasia in CRS, is unknown.

Therefore, the purpose of this study was to analyze the tissues of patients with CRS and to investigate the effects and regulatory mechanisms of S100A8 and S100A9 on tissue remodeling in human nasal epithelium, especially squamous metaplasia, through bulk RNA sequencing analysis with HNE cell culture.

II. MATERIALS AND METHODS

1. Participants

This study was reviewed and approved by the appropriate institutional review boards (IRB) and ethics committees (No. 2020-05-004). Written informed consent was obtained from all of the patients prior to enrollment in this study. All of the procedures in the studies involving human participants were performed in accordance with the ethical standards of the institutional and/or national research committee and with the 1964 Helsinki declaration and its later amendments or comparable ethical standards.

The patients who participated in this study were adults 19 years or older, and the control groups were patients who underwent middle meatal antrostomy due to a lesion confined to the maxillary sinus. After confirming the ethmoid mucosal condition with preoperative CT and surgical findings, ethmoid mucosa was harvested. CRS was diagnosed and classified based on the 2020 European position paper on rhinosinusitis and nasal polyps[24]. Patients who had malignancy, pregnancy, chronic renal/cardiac diseases, and/or immunosuppression were excluded, and all of the patients stopped taking intranasal or oral steroids one month before surgery.

The disease severity of CRS was based on Lund-Mackay scores, which is a well-known method that calculates scores for each side according to CT findings and combines the two scores to obtain the final score[25]. The olfactory function was measured using the YSK olfactory function test kit (YOF test; Kimex Co., Suwon, Korea) before surgery, and the sum of the threshold, discrimination, and identification scores was defined as the olfactory function score, as with previously reported methods[26]. In addition, demographic data, including age, sex, underlying diseases (e.g., allergies and asthma), and the sino-nasal outcome test (SNOT) 22 score, were analyzed.

2. Cell culture

HNE cell culture was performed as previously described[27,28]. HNE cells were isolated from a nasal polyp obtained from a patient who underwent endoscopic sinus surgery for

CRS. Passage-2 HNE cells were prepared, and $1x10^5$ HNE cells were seeded in 0.5 mL of culture medium on 24.5 mm, 0.45 μm pore size, Trans well-clear (Costar Co., Cambridge, MA, USA) culture inserts. Cells were cultured in a 1:1 mixture of bronchial epithelial growth medium that comprised Dulbecco's modified Eagle's medium with all of the supplements as described. The cells were grown and submerged for the first nine days, and the culture medium was changed on day 1 and every other day thereafter. We created an air-liquid interface (ALI) on day 9 by removing the apical medium and restricting the culture feeding to the basal compartment. A 37 °C humidified cell incubator infused with filtered air was used to differentiate HNE cells into ciliated respiratory epithelial cells. On the 14th ALI day, 10 μg/mL of lipopolysaccharide (LPS), 10 μg/mL of house dust mites (HDM), and 5 ng/mL of β-glucan were treated; these were harvested after one day. In addition, in order to examine the expression of S100A8 and S100A9 according to type 1 (TNF-α, IFN-γ, IL-1β) and type 2 cytokines (IL-4, IL-13), samples were harvested on days 1, 2, and 3 after the administration of each cytokine by 10 ng/mL. Finally, to investigate the effect of S100A8, S100A9, and calprotectin on HNE cells, samples were collected after each recombinant protein was treated for one and three days.

3. RNA isolation and real-time quantitative polymerase chain reaction (PCR)

Total RNA was isolated from HNE cells using TRIzol (Invitrogen, Carlsbad, CA, USA) according to the manufacturer's protocol. cDNA was synthesized with random hexamers (PerkinElmer Life Sciences, Waltham, MA, USA) using the Moloney murine leukemia virus reverse transcriptase (PerkinElmer Life Sciences; Waltham, MA, USA). Real-time quantitative PCR (qPCR) was carried out using a 7300 Fast Real-Time PCR System with SYBR Green PCR Core Reagents (Applied Biosystems, Foster City, CA, USA) according to the manufacturer’ s protocols. Reactions were performed in a total volume of 20 μl, which included 10 μl of 2x SYBR Green PCR Master Mix, 0.5 μl of each primer, 7 μl of three-time autoclaved distilled water, and 2 μl of previously reverse-transcribed cDNA template. The qPCR primers were designed based on the GenBank sequences:

S100A8 (Forward 5'-AAT TTC CAT GCC GTC TAC AG-3', Reverse 5'-CGC CCA TCT TTA TCA CCA G-3'), *S100A9* (Forward 5'-AAA AGG TCA TAG AAC ACA TCA TGG-3', Reverse 5'-GAA GCT CAG CTG CTT GTC TG-3'), *Involucrin* (Forward 5'-TGT TCC TCC TCC AGT CAA TAC C-3', Reverse 5'-TCC CAG TTG CTC ATC TCT CTT G-3'), *MMP9* (Forward 5'-GCC GAC TTT TGT GGT CTT CC-3', Reverse 5'-TAC AAG TAT GCC TCT GCC AGC-3'), and *β-actin* (Forward 5'-GCC AAC CGC GAG AAG ATG-3', Reverse 5'-ACG GCC AGA GGC GTA CAG-3'). The thermal cycler was set to perform 40 cycles of the following: denaturation at 95 °C for 30 seconds, annealing at 60 °C for 30 seconds, and finally, polymerization at 95 °C for 15 seconds. Melting curve analysis was performed to confirm the specificity of the amplified PCR products. The relative quantity of each target mRNA was normalized against β-actin as an endogenous control. The mRNA expression was obtained using the comparative cycle threshold (Ct) method.

4. Histopathology and immunohistochemistry

Tissues obtained from the patients who underwent endoscopic sinus surgery were fixed with 10% formalin for at least 24 hours. All of the fixed tissues were embedded in paraffin. Each paraffin block was sliced into 4-μm-thick sections. Sliced specimens were prepared for histological analysis with haematoxylin and eosin (H&E) staining.

Immunohistochemistry was performed using the BenchMark ULTRA automated slide stainer combined with VENTANA detection kits (Ventana Medical Systems, Tucson, AZ, USA), following the manufacturer’ s protocol. After deparaffinization, the slides were treated for four minutes at room temperature with the peroxidase inhibitor included in the detection kit without antigen retrieval to inhibit endogenous peroxidase. The first antibody reaction was incubated for 28 minutes at 36 °C with a rabbit monoclonal anti-S100A8 antibody (Abcam, Cambridge, UK), a rabbit polyclonal anti-S100A9 antibody (Abcam), a mouse monoclonal anti-calprotectin antibody (Abcam), and a mouse monoclonal anti-Involucrin antibody (Thermo Fisher Scientific Inc., Waltham, MA,

USA). The negative control was incubated with nonimmune serum rather than with the primary antibody. In addition, the sections were incubated in the OptiView DAB IHC Detection Kit solution (Ventana Medical Systems) for eight minutes. Counterstaining and post-counterstain were performed for four minutes using hematoxylin and bluing reagent.

Epithelial remodeling was classified into normal epithelium, epithelial hyperplasia, goblet cell hyperplasia, and squamous metaplasia according to the previously described method[29,30]. Tissue analysis was performed by a pathologist using an Olympus U-TV0.63XC light microscope. S100A8 and S100A9 intensity analyses for immunohistochemistry were performed with Image J software (version 1.53a; National Institutes of Health, Bethesda, MD, USA).

5. Immunofluorescence

Paraffin-embedded tissue slides were deparaffinized and rehydrated. After antigen retrieval, the tissue sections were blocked for one hour at room temperature with 5% bovine serum albumin. The primary antibody reaction was incubated overnight at 4 °C in a humidified chamber. The primary antibodies were a rabbit monoclonal anti-S100A8 antibody (Abcam), a rabbit polyclonal anti-S100A9 antibody (Abcam), and a mouse monoclonal anti-Involucrin antibody (Thermo Fisher Scientific Inc.). Subsequently, the secondary antibody reaction was incubated at room temperature for 30 minutes using Alexa Fluor 488 goat anti-mouse Ig G polyclonal secondary antibodies (Invitrogen) and Alexa Fluor 568 goat anti-rabbit IgG polyclonal secondary antibodies (Invitrogen). All of the negative controls were immunostained with nonimmune serum rather than with primary antibodies. In addition, nucleic acids were stained with 4′,6-diamidino-2-phenylindole (i.e., DAPI, Invitrogen). Finally, coverslips were mounted onto the slides with fluorescent mounting media (DAKO, Glostrup, Denmark). Fluorescence images were obtained with a Zeiss LSM 700 confocal laser scanning microscope (Carl Zeiss, Berlin, Germany) and analyzed using the ZEISS ZEN 3.2 blue edition (Carl Zeiss).

6. Western blot

HNE cells were lysed using 2x lysis buffer (250 mM Tris-HCl at pH 6.5, 2% sodium dodecyl sulfate [SDS], 4% mercaptoethanol, 0.02% bromphenol blue, and 10% glycerol) with a phosphatase inhibitor cocktail (Thermo Fisher Scientific, Rockford, IL, USA) on ice. Equal amounts of whole cell lysates were electrophoresis on 8% or 12% SDS-polyacrylamide gel and transferred to a polyvinylidene difluoride membrane (Millipore; Bedford, MA, USA). Membranes were blocked with 5% skim milk in Tris-buffered saline (50 mM Tris-HCl and 150 mM NaCl at pH 7.5) for two hours at room temperature. The blot was incubated overnight with primary antibodies, including S100A8 (Abcam), S100A9 (Abcam), Involucrin (Thermo Fisher Scientific Inc.), MMP9 (Abcam), and β-actin (Santa Cruz, CA, USA) in 0.5% Tween 20 in Tris-buffered saline (TTBS). After three washes with TTBS, the blot was further incubated for 45 minutes at room temperature with an anti-rabbit or -mouse secondary antibody in TTBS and was visualized using the ECL kit (Amersham, Little Chalfont, Buckinghamshire, UK). Each target sample was normalized based on β-actin. The analyzing of relative band intensity was measured with the Image J program (version 1.53a; National Institutes of Health, Bethesda, MD, USA).

7. Bulk RNA sequencing and data analysis

Total RNA was isolated from HNE cells treated with recombinant S100A8, S100A9, and calprotectin using a TRIzol reagent (Invitrogen, Gaithersburg, MD, USA) according to the manufacturer's protocol. The collected total RNA samples were stored at -80 °C and delivered to Macrogen Inc. (Seoul, South Korea). The delivered samples were subjected to sample quality control, library quality control, and data analysis according to the manufacturer's instructions. Sample quality and quantity RNA was checked using the 2100 Bioanalyzer. DNA contamination was removed using DNase. To determine the size of PCR-enhanced fragments, template size distribution was verified by running on an

Agilent Technologies 2100 Bioanalyzer using a DNA 1000 chip. The purified RNA was randomly fragmented for short read sequencing. The fragmented RNA fragment was converted into cDNA through the reverse transcription process. Different adapters were attached to both ends of the created cDNA fragment and were ligated. After PCR amplification to the extent possible for sequencing, an insert size of 200–400 bp was obtained through the size selection process.

For data analysis, reads that had undergone pre-processing were mapped to the reference genome using the HISAT2 program. Aligned reads were then generated. Transcript assembly was performed through the StringTie program using the reference-based aligned reads information. Expression profiles were extracted with Fragments Per Kilobase of Transcript per Million mapped reads (FPKM)/Reads Per Kilobase of transcript per Million mapped reads (RPKM) and Transcripts per Kilobase Million (TPM). A list of significant differentially expressed genes (DEGs) set enrichment analyses was performed using gProfiler (https://biit.cs.ut.ee/gprofiler/orth), which contained a functional classification of gene ontology, including the biological process, molecular function, and cellular component. In addition, ingenuity pathway analysis (IPA) was conducted by Professor Eun-Jeong Lee of the Yonsei University College of Medicine, Wonju, based on bulk RNA sequencing data.

8. Statistical analyses

All of the statistical analyses were performed using IBM SPSS Statistics 26.0 (IBM Corp., Armonk, NY, USA). Continuous data are expressed as mean ± standard deviation, Unpaired Student’ s t-test and one-way ANOVA were used to analyze the data. Pearson’ s correlation coefficients were calculated between the clinical data and immunohistochemistry intensity. A p value of less than 0.05 was considered statistically significant.

III. RESULTS

1. Responses of S100A8 and S100A9 in HNE cells to external stimuli

A. Treatment with LPS, HDM, and β-glucan

Preliminary data for S100A8 and S100A9 were obtained from bulk RNA sequencing data, which was performed after HNE cells were treated with LPS, HDM, and β-glucan. In particular, when LPS was applied, S100A8 and S100A9 showed an increase at the gene level (data not shown). Based on the bulk RNA sequencing data, experiments were redone for qPCR and western blot. As a result, as with the bulk RNA sequencing data, S100A8 and S100A9 increased when LPS was applied (Figure 1). In short, these results confirmed that S100A8 and S100A9 increase when inflammatory mediators, such as LPS, are induced

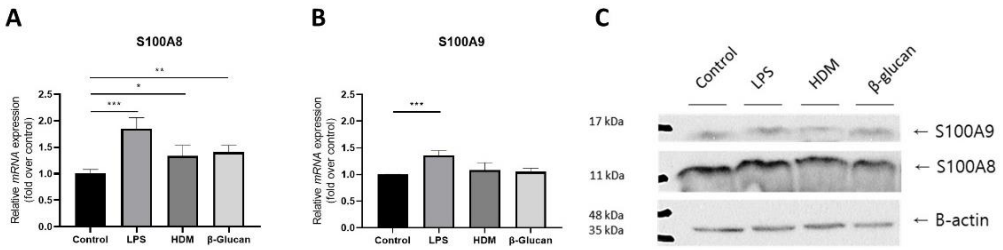

Figure 1. qPCR and western blot of S100A8 and S100A9 in HNE cells treated with LPS, HDM, and β-glucan.

B. Response for type I cytokines and type II cytokines

Based on the finding that S100A8 and S100A9 are increased by LPS, we tried to confirm the response of S100A8 and S100A9 under the conditions of pro-inflammation by type I cytokines and anti-inflammation by type II cytokines. Among type 1 cytokines, in particular, when TNF-α and IL-1β were applied, the gene level of S100A8 and S100A9

increased by day one, and their protein levels increased by day three (Figures 2 and 3). On the other hand, when IL-4 and IL-13, known as type II cytokines, were applied, the gene and protein levels of S100A8 and S100A9 decreased over time. Based on these results, it was hypothesized that S100A8 and S100A9 in HNE cells increased due to pro-inflammatory conditions and would have any effect on HNE cells.

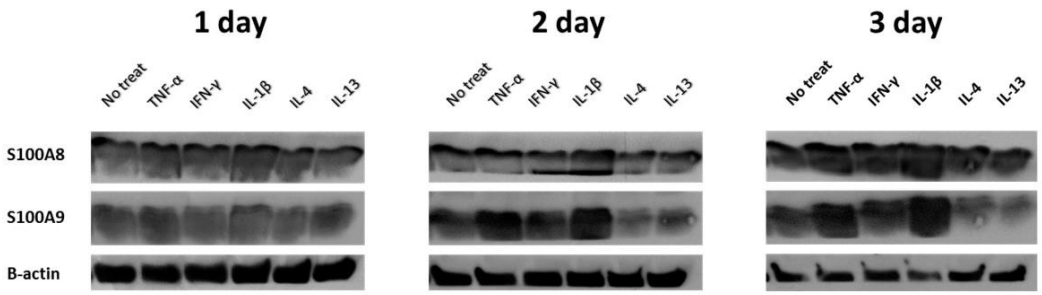

Figure 2. Western blot of S100A8 and S100A9 in HNE cells treated with types 1 and 2 cytokines

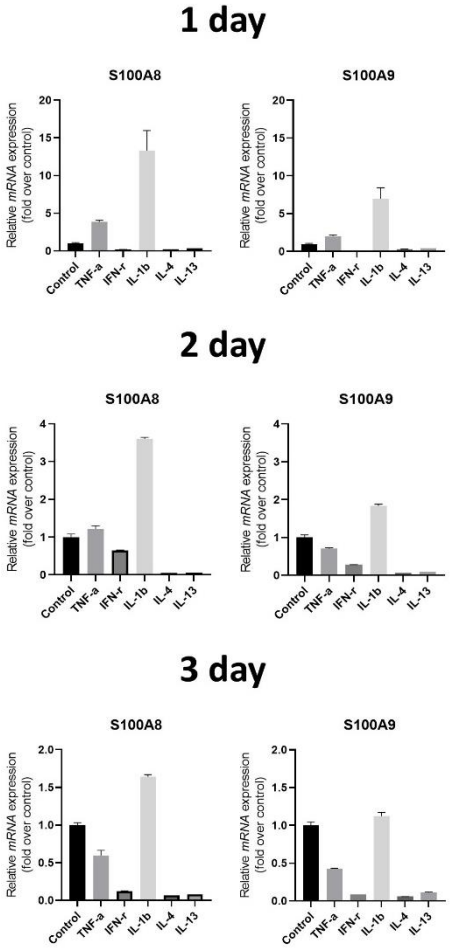

Figure 3. qPCR of S100A8 and S100A9 in HNE cells treated with types 1 and 2 cytokines

2. Expression analysis of S100A8 and S100A9 in the epithelium of CRS tissue

A. Human sample demographic data

To investigate the role of S100A8 and S100A9 by inflammation in HNE cells, we analyzed the tissues of patients with CRS, which was represented by chronic inflammation. As a result of analyzing the tissues of 9 healthy controls, 21 patients with CRS without nasal polyps (CRSsNP), and 32 with CRS with nasal polyps (CRSwNP),

tissue remodeling was found to be dominant in the patients with CRSwNP, and squamous metaplasia was particularly prominent in those with CRSwNP (Table 1).

Table 1. Demographic data

	Control (n=9)	**CRSsNP (n=21)**	**CRSwNP (n=32)**
Gender (female/male)	7/2	3/18	7/25
Age, years	61.2±11.4	54.3±12.6	47.1±13.6
Smoke, (n)	3	14	18
Allergy, (n)	1	10	19
Asthma, (n)	0	2	6
Olfactory function score	23.6±5.3	19.1±9.3	19.3±9.9
SNOT 22	27.8±15.0	29.6±18.9	40.3±20.2
Lund-Mackay score	1.4±1.1	9.6±4.0	13.2±5.9
ECRS, (n)	0	12	19
Epithelial structure[#]			
Normal epithelium	3	4	1
Epithelial hyperplasia	1	3	25
Mucous hyperplasia	5	14	9
Squamous metaplasia	0	0	16

[#]Analysis by pathologist

Abbreviations: CRSsNP; chronic rhinosinusitis without nasal polyp, CRSwNP; chronic rhinosinusitis with nasal polyp, SNOT; sino-nasal outcome test, ECRS; eosinophilic chronic rhinosinusitis,

As a result of immunohistochemistry of S100A8 and S100A9, it was confirmed that they were strongly expressed in squamous epitheliums (Figure 4).

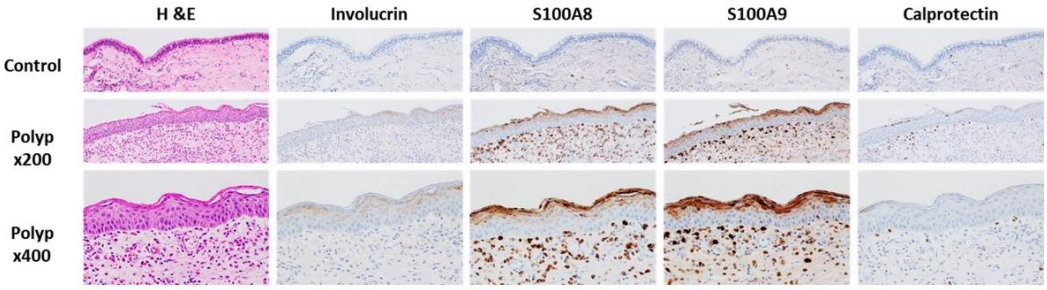

Figure 4. Immunohistochemistry of S100A8, S100A9, and calprotectin in patients with CRSwNP

In addition, it was confirmed that S100A8 and S100A9 co-localized with Involucrin, a representative marker of squamous metaplasia, through immunofluorescence (Figure 5). As a result of analyzing the intensities for the immunohistochemistry of S100A8 and S100A9, the CRSwNP group showed a more increased expression than the control and CRSsNP groups; it was found that expressions of them were particularly high in squamous metaplasia lesions (Figure 6). In addition, as the intensities of S100A8 and S100A9 in the tissues increased, SNOT 22, an index of clinical symptoms, was found to increase and showed a positive correlation with the Lund-Mackay score. These results suggested that the increase in S100A8 and S100A9 in nasal epithelium could be an index reflecting the severity of CRS (Figure 7). However, it was not known whether S100A8 and S100A9 were the cause or the result of squamous metaplasia; thus, an experiment was needed to confirm the cause and effect.

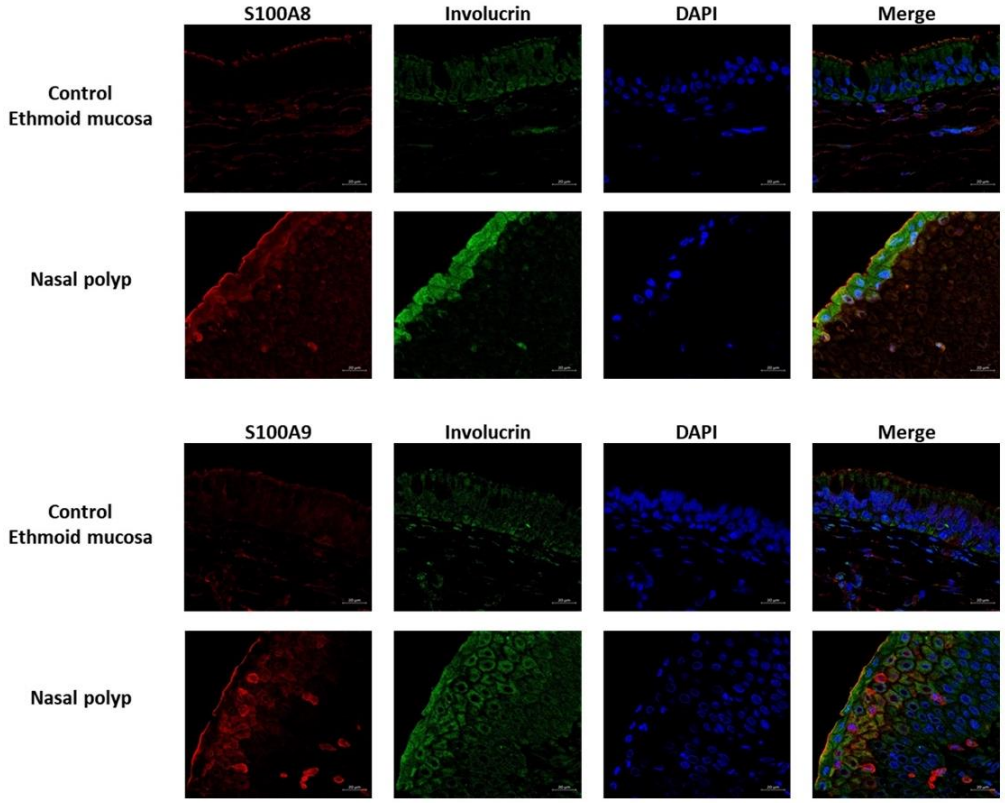

Figure 5. Immunofluorescence of S100A8 and S100A9 in normal ethmoid mucosa and nasal polyps

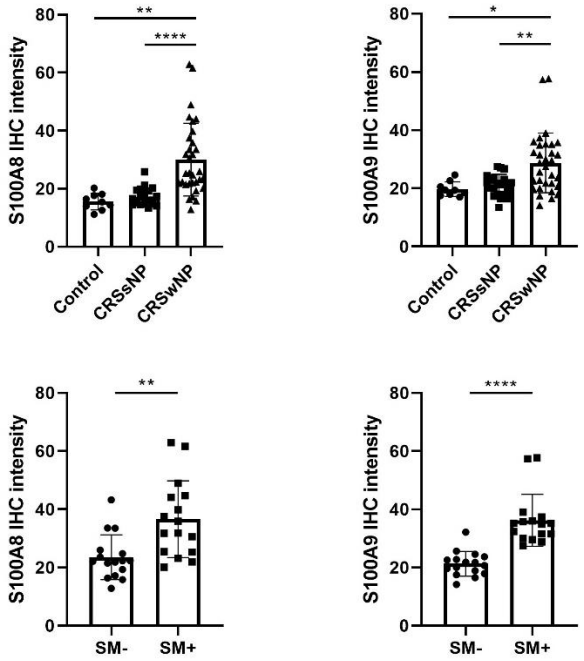

Figure 6. Immunohistochemistry intensity of S100A8 and S100A9 in tissue

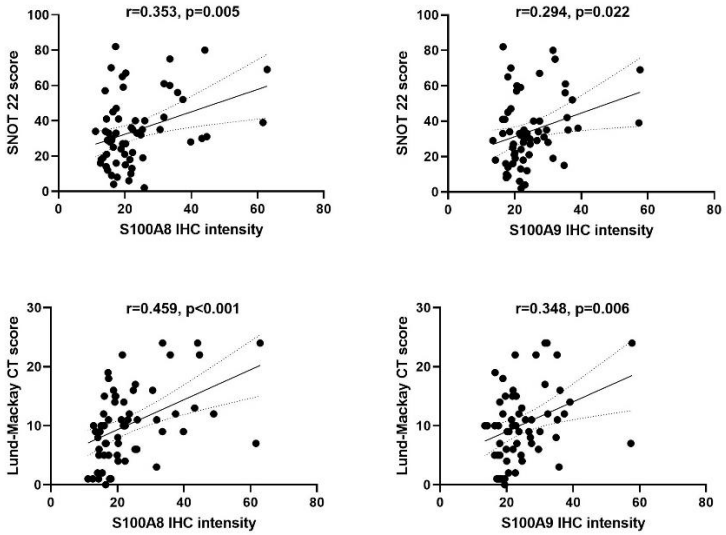

Figure 7. Correlations between immunohistochemistry intensity and clinical findings

3. Conditional experiment for bulk RNA sequencing

A. Confirmation of squamous metaplasia and tissue remodeling

To determine whether S100A8 and S100A9 and their complex, calprotectin, affect tissue remodeling, particularly squamous metaplasia, in cultured HNE cells through bulk RNA sequencing. First, a conditional experiment was conducted (Figure 8).

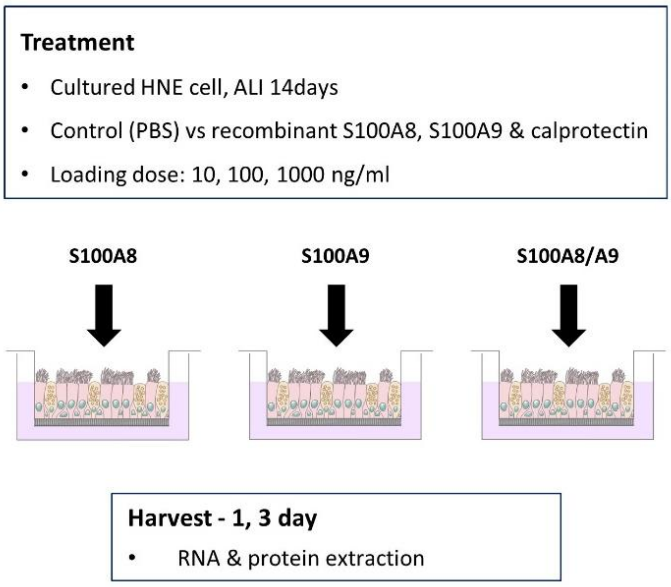

Figure 8. Scheme of a conditional experiment for effects of S100A8, S100A9, and calprotectin on HNE cells

To check the appropriate concentration and time point, recombinant S100A8, S100A9, and calprotectin were used. Experimental conditions were confirmed with Involucrin, one of the markers of squamous metaplasia, and MMP9, a representative marker of tissue remodeling. In RT-PCR, all of them showed increased findings at day three rather than at day one, and in particular, when 100 ng/mL of each protein was administered, the most increased findings were observed (Figure 9).

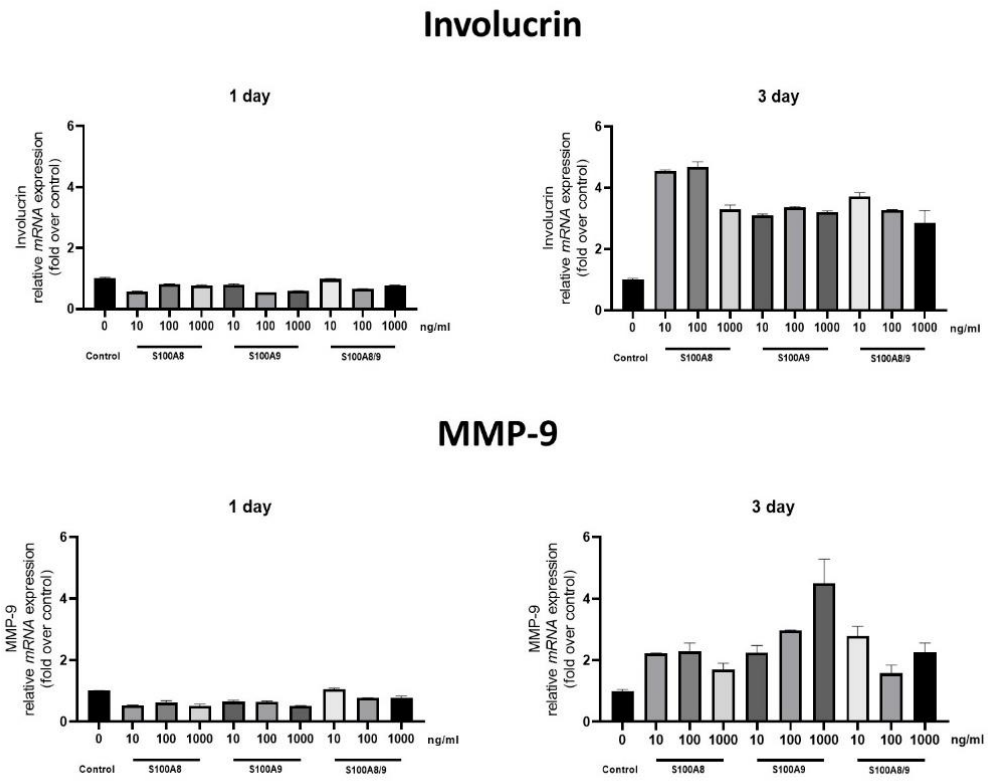

Figure 9. qPCR results for treatment with recombinant S100A8, S100A9, and calprotectin on HNE cells

In addition, it was confirmed via the western blot that tissue remodeling and squamous metaplasia marker proteins increased. In particular, Involucrin and MMP9 were more greatly increased when S100A9 was applied than when S100A8 and calprotectin were administered (Figure 10). Therefore, 100 ng/mL of each recombinant protein was treated in the cultured HNE cells and harvested on the third day, followed by bulk RNA sequencing analysis.

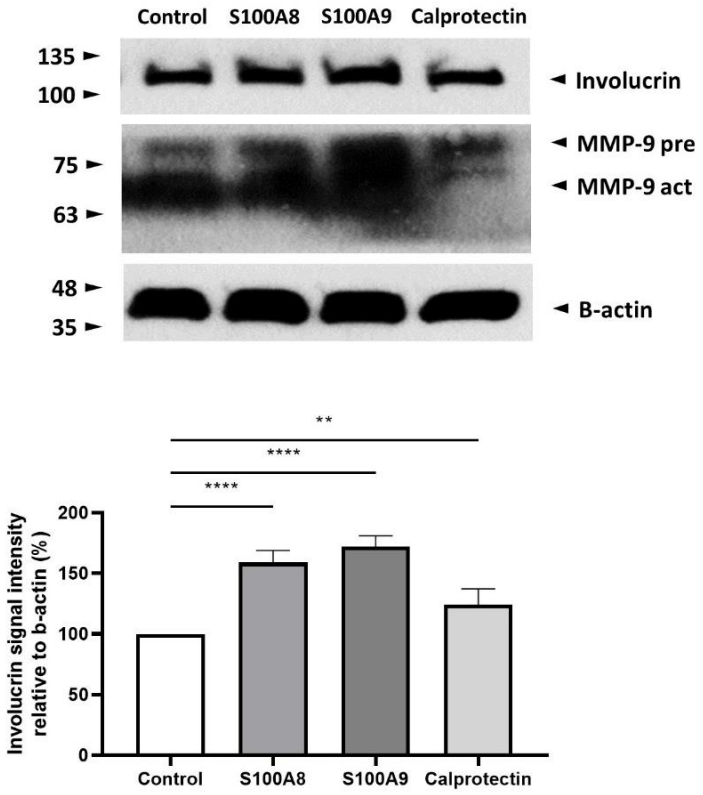

Figure 10. Western blot applied to recombinant S100A8, S100A9, and calprotectin on HNE cells

4. Bulk RNA sequencing data analysis

A. Comparisons among three groups

After each recombinant protein was treated with HNE cells on day 14 of ALI, four samples per group were analyzed for bulk RNA sequencing analysis. Through a one-way hierarchical clustering heatmap analysis, S100A8 and S100A9 showed similar findings, but it was confirmed that the two groups were different from the control group (Figure 11).

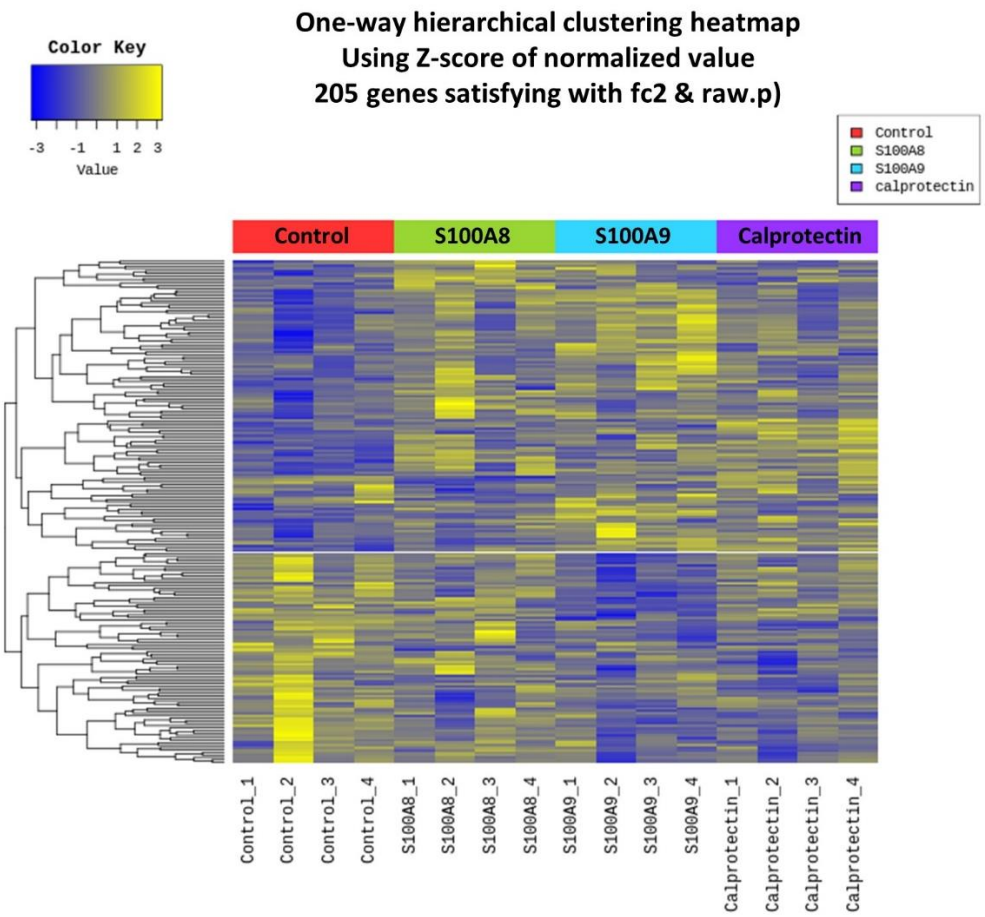

Figure 11. Hierarchical clustering heatmap analysis for S100A8, S100A9, and calprotectin

On the other hand, it was confirmed that the group administered with calprotectin was different from the control group and from the S100A8 and S100A9 groups. When S100A8 was applied, 39 genes increased and 17 genes decreased compared to that of the control group. S100A9 also showed the most gene changes, with 62 genes increasing and 59 genes decreasing. In the group administered with calprotectin, 26 genes increased and 37 genes decreased (Figure 12). Through the Venn diagram, it was possible to identify the increased and decreased genes in the three groups (Figure 13).

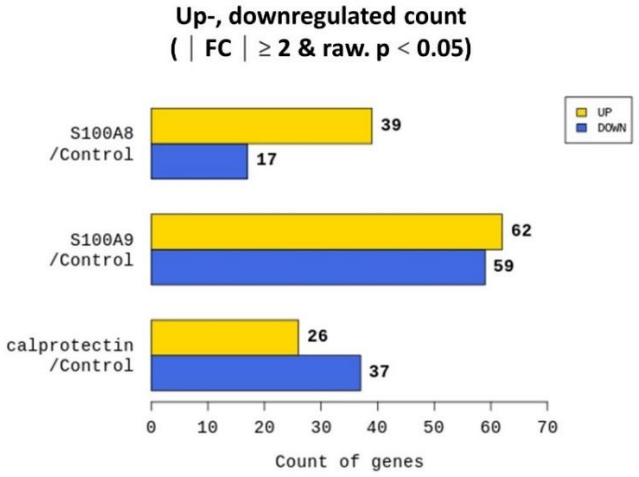

Figure 12. Count of genes after treatment with S100A8, S100A9, and calprotectin

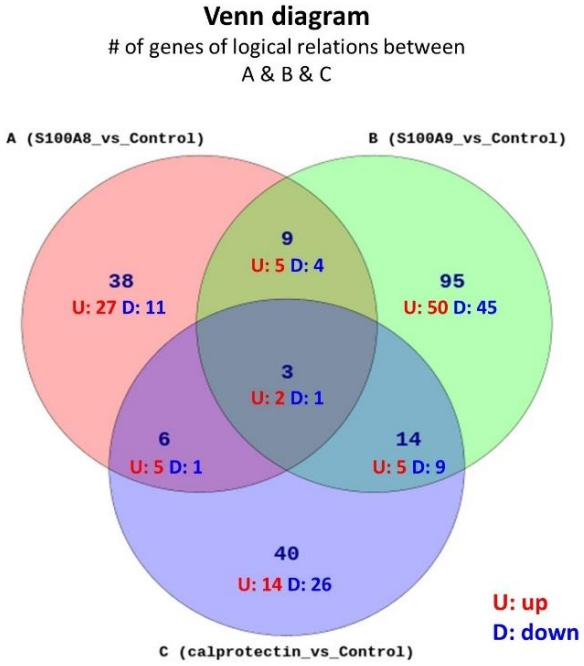

Figure 13. Venn diagram for S100A8, S100A9, and calprotectin

Gene ontology functional group analysis revealed that the effects of S100A8, S100A9, and calprotectin on HNE cells were slightly different. In the biological process, calprotectin was mainly shown to respond to xenobiotics, and S100A8 was shown to be involved in the metabolic process. On the other hand, S100A9 was found to be involved in keratinization, keratinocyte differentiation, and epidermal cell differentiation (Figure 14).

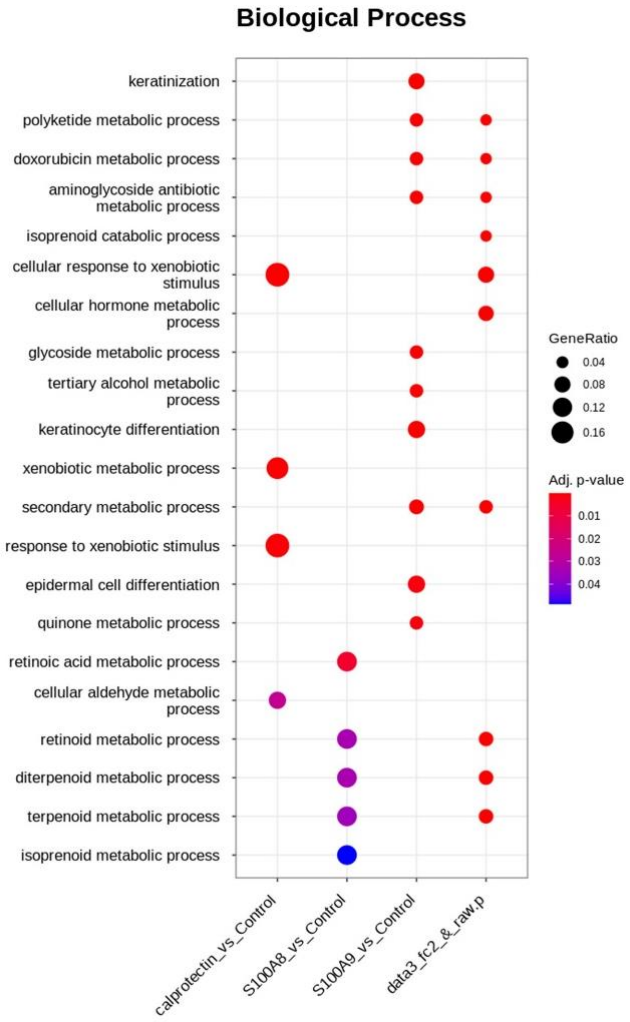

Figure 14. Biological process in gene ontology functional group analysis

As for the cellular component, it was found that S100A9 was involved in the development of the cornified envelope associated with squamous metaplasia and the collagen-containing extracellular matrix involved in tissue remodeling (Figure 15).

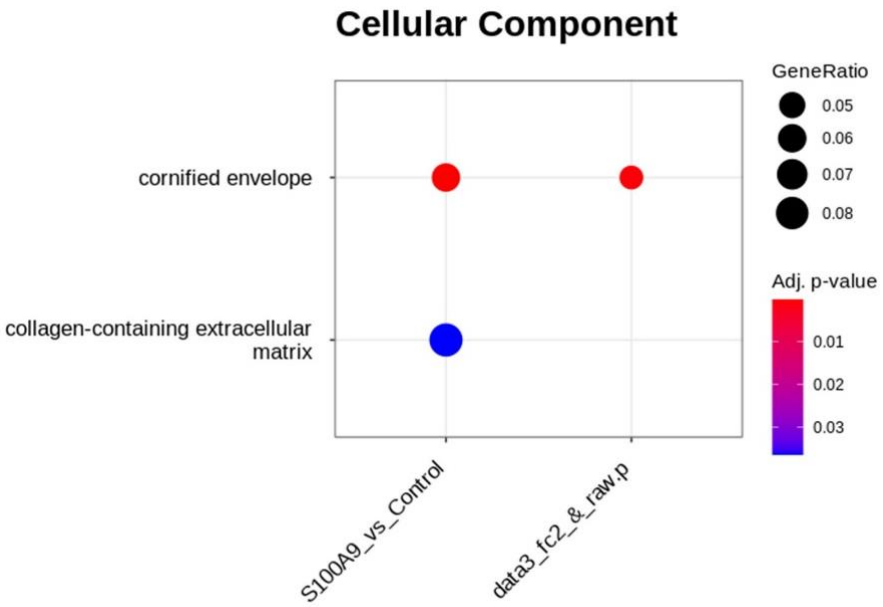

Figure 15. Cellular component in gene ontology functional group analysis

Furthermore, it was confirmed that there was a difference between S100A8, S100A9, and calprotectin in molecular function analysis (Figure 16). As a result, while it was known that the functions of these three proteins are similar, the similarities and differences between each protein were confirmed through bulk RNA sequencing analysis.

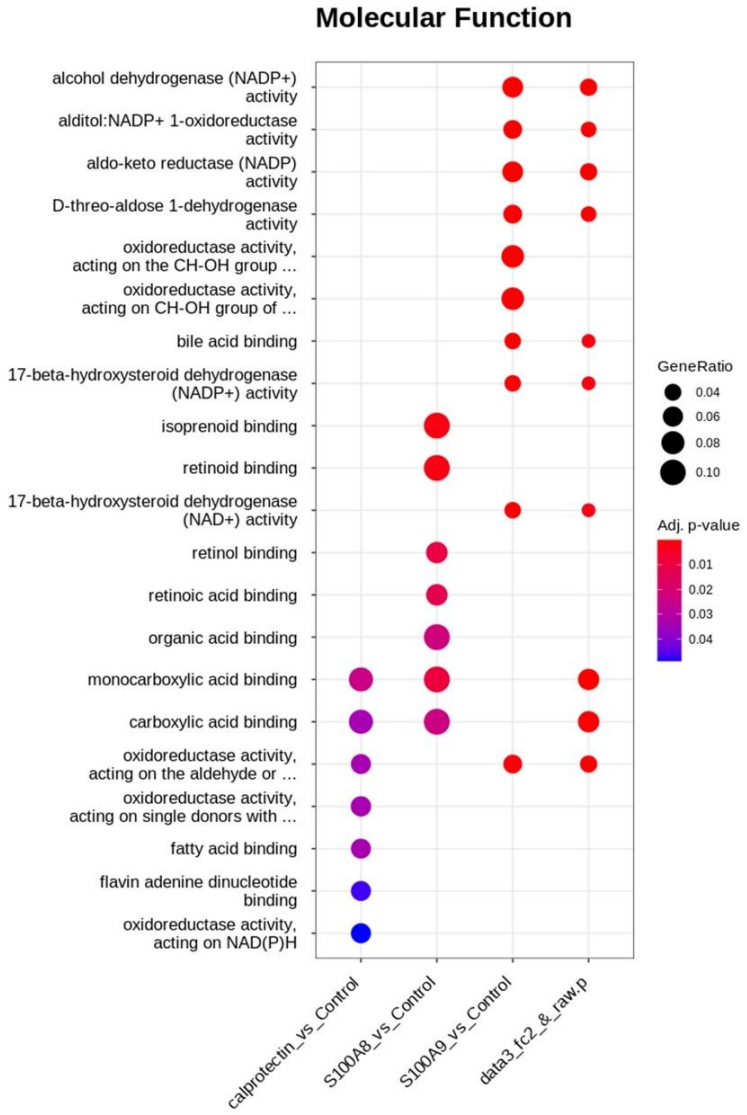

Figure 16. Molecular function in gene ontology functional group analysis

B. Ingenuity pathway analysis (IPA) for effects of S100A8, S100A9, and calprotectin

(A) Upstream regulator list and downstream effects analysis

In order to prove the hypothesis that S100A8 and S100A9 are involved in tissue remodeling and squamous metaplasia, an additional in-depth analysis was conducted based on bulk RNA sequencing data derived from S100A9 treatment (Figures 17 and 18).

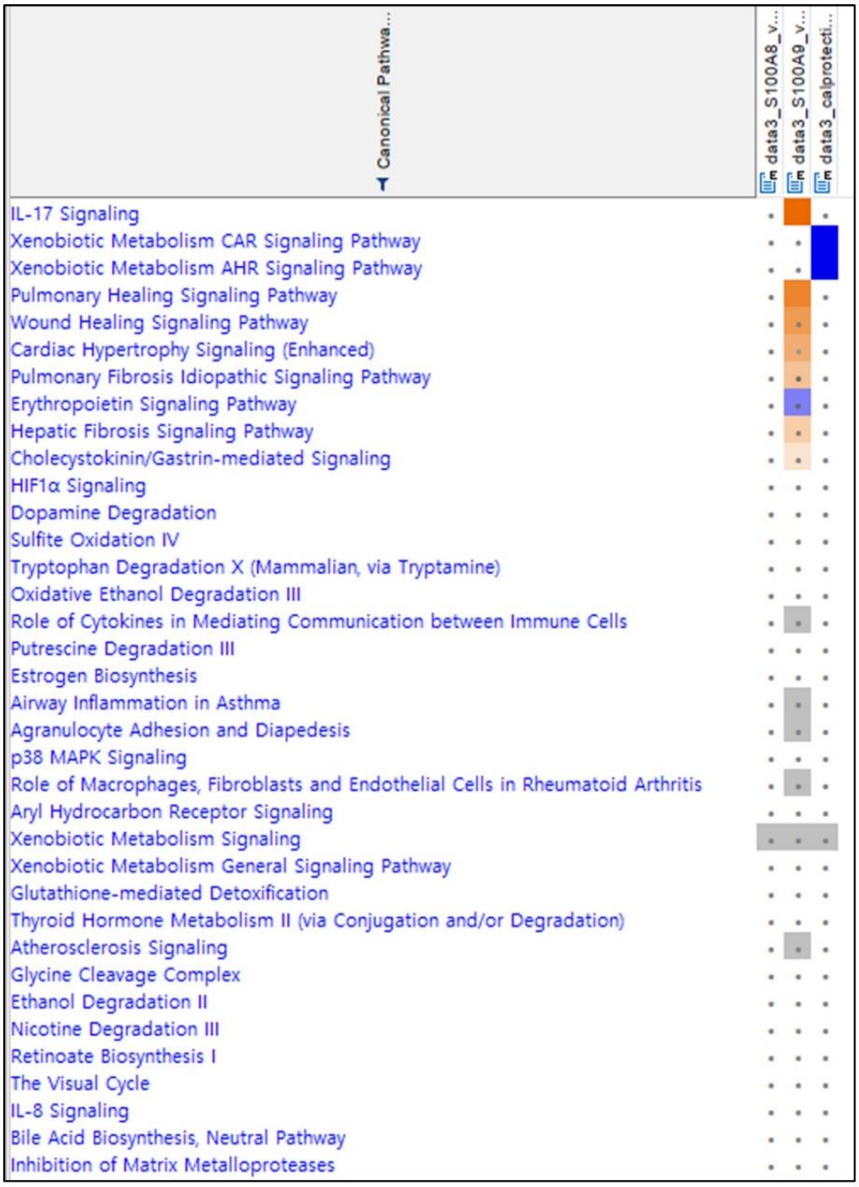

Figure 17. Ingenuity pathway analysis (IPA) for S100A8, S100A9, and calprotectin

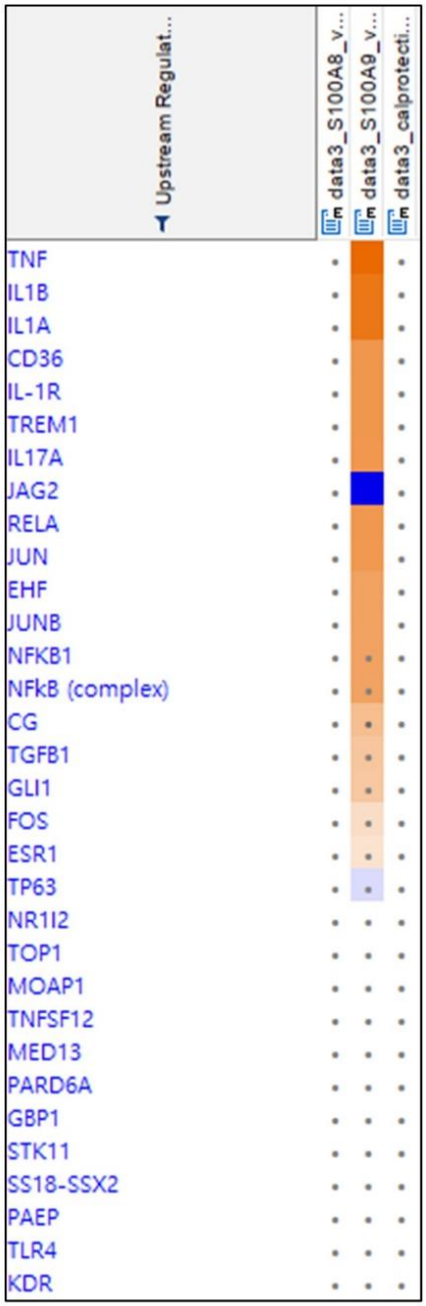

Figure 18. Upstream regulator molecule analysis for S100A8, S100A9, and calprotectin

The target molecule of the upstream regulator affected the increase of genes involved in IL-17 signaling (*e.g.*, *CCL20*, *CXCL3*, *CXCL5*, *IL33*, *IL17C*, and *IL36B*) and in *MMP1* and *MMP10*, which are genes related to tissue remodeling, and was shown to affect the expression of *SPRR2A* and *SPRR2B* related to squamous metaplasia (Table 2). In addition, a downstream effects analysis was performed to analyze genes affected by S100A9. As a result, as shown in Table 3, *MMP1*, a tissue remodeling marker, and *SPRR2A*, a squamous metaplasia marker, were included in the top gene.

Table 2. Upstream regulator gene list for S100A9 vs. control group

Upstream regulator	Molecule type	Predicted activation state	Activation z-score	p-value of overlap	Target molecules in dataset
TNF	cytokine	Activated	3.208	0.00001	*BCL2A1, CCL20, CXCL3, CXCL5, DPP4, IL17C, IL33, IL7R, MMP1, MMP10, PI3*
IL1B	cytokine	Activated	2.93	0.00000	*BCL2A1, CCL20, CXCL3, CXCL5, DPP4, IL36B, MMP1, MMP10, SERPINA3*
IL1A	cytokine	Activated	2.926	2.42E-10	*CCL20, CXCL3, CXCL5, MMP1, MMP10, PI3, SERPINA3, SPRR2A, SPRR2B*
IL-1R	group	Activated	2.236	5.08E-07	*CCL20, CXCL3, CXCL5, MMP1, MMP10*
CD36	transmembrane receptor	Activated	2.236	9.59E-07	*CCL20, CXCL3, CXCL5, MMP1, MMP10*
TREM1	transmembrane receptor	Activated	2.236	0.00071	*CCL20, CXCL3, CXCL5, MMP1, MMP10*
IL17A	cytokine	Activated	2.224	0.00002	*BCL2A1, CCL20, CXCL3, CXCL5, MMP1*
RELA	transcription regulator	Activated	2.211	0.00036	*ANKRD1, CCL20, CXCL3, CXCL5, MMP1, PI3*
JUN	transcription regulator	Activated	2.191	0.00001	*ANKRD1, CCL20, CXCL3, CXCL5, IL7R, MMP1, MMP10*
JUNB	transcription regulator	Activated	2	0.00004	*CCL20, CXCL3, MMP1, MMP10*
EHF	transcription regulator	Activated	2	0.00025	*CCL20, SERPINA3, SPRR2A, SPRR2E*

Table 3. Downstream effects analysis for S100A9 vs. control group

Genes in dataset	Prediction	Fold change	Related findings
MMP1	Affected	2.52	Affects (2)
CCL20	Affected	2.516	Affects (14)
CXCL5	Affected	2.404	Affects (2)
SPRR2A	Affected	2.314	Affects (1)
BCL2A1	Affected	2.216	Affects (1)
FGFR1	Affected	2.149	Affects (10)
IL33	Affected	2.143	Affects (3)
IL7R	Affected	2.093	Affects (1)
DPP4	Affected	2.073	Affects (1)
CXCL3	Affected	2.051	Affects (1)
L1CAM	Affected	2.043	Affects (1)
PHACTR3	Affected	-2.022	Affects (1)
LY6G6C	Affected	-2.094	Affects (1)
SNORD3A	Affected	-2.1	Affects (1)
OCA2	Affected	-2.16	Affects (2)
KLK14	Affected	-2.357	Affects (1)
MEF2B	Affected	-4.898	Affects (1)
TGM3	Affected	-6.116	Affects (1)

C. Gene ontology functional analysis for effects of S100A9

(A) Biological process

To investigate the effect of S100A9 on HNE cells, bulk RNA sequencing was performed, followed by gene ontology functional analysis. As a result, the top 20 items involved in biological processes are shown in Figure 19. Among the top items, epidermis development, keratinocyte differentiation, epidermal cell differentiation, skin

development, and keratinization were included. As shown in Table 4, the genes included in these items were *SPRR2A*, *SPRR2B*, *SPRR2E*, *SPRR2F*, *TMG3*, *LIPN*, *AKR1C3*, and *KLK14*.

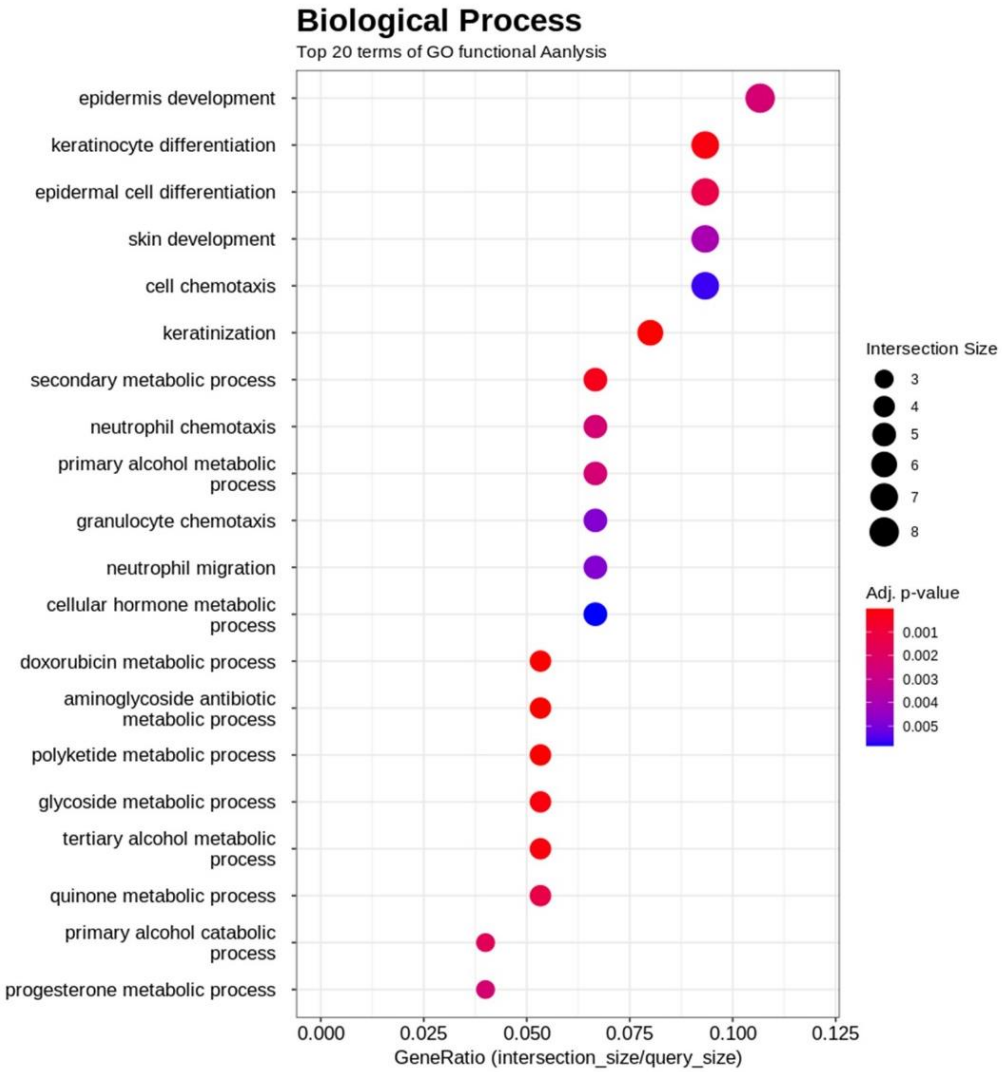

Figure 19. Biological process in gene ontology for S100A9

(B) Cellular component

S100A9 is a cellular component affecting HNE cells, and the top two items were detected. One was a collagen-containing extracellular matrix and the other, a cornified envelope (Figure 20). Genes related to the former were *VWF*, *L1CAM*, *AMTN*, *SERPINA3*, *COL21A1*, *FREM1*, and *HMCN1*, and genes related to the extracellular matrix were *PI3*, *VWF*, *L1CAM*, *AMTN*, *SERPINA3*, *MMP1*, *GPLD1*, *COL21A1*, *MMP10*, *FREM1*, and *HMCN1*, with a statistically significant difference (adjusted p value = 0.0005, Table 4). On the other hand, genes included in the latter were *SPRR2A*, *SPRR2B*, *SPRR2E*, *SPRR2F*, and *PI3*, which were associated with squamous metaplasia. Genes related to squamous metaplasia were similarly increased when S100A8 was applied.

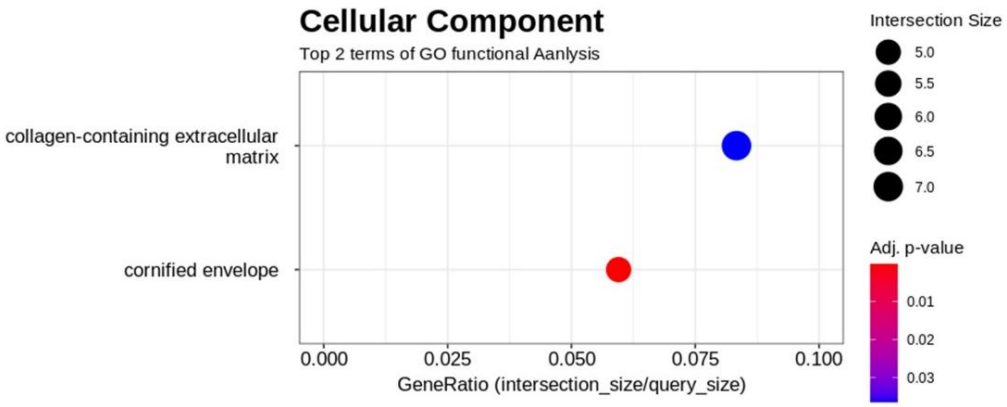

Figure 20. Cellular component in gene ontology for S100A9

Table 4 Gene ontology analysis of S100A9 vs. control group

Source	Gene ID	Function	Related genes	P-value
BP	0031424	keratinization	*SPRR2B, SPRR2A, LIPN, SPRR2F, TGM3, SPRR2E*	4.49E-05
BP	0030216	keratinocyte differentiation	*SPRR2B, SPRR2A, LIPN, SPRR2F, TGM3, AKR1C3, SPRR2E*	0.000195
BP	0009913	epidermal cell differentiation	*SPRR2B, SPRR2A, LIPN, SPRR2F, TGM3, AKR1C3, SPRR2E*	0.001309
BP	0008544	epidermis development	*SPRR2B, SPRR2A, LIPN, SPRR2F, TGM3, AKR1C3, KLK14, SPRR2E*	0.002405
BP	0043588	skin development	*SPRR2B, SPRR2A, LIPN, SPRR2F, TGM3, AKR1C3, SPRR2E*	0.003984
CC	0001533	cornified envelope	*SPRR2B, PI3, SPRR2A, SPRR2F, SPRR2E*	8.79E-05
CC	0062023	collagen-containing extracellular matrix	*VWF, L1CAM, AMTN, SERPINA3, COL21A1, FREM1, HMCN1*	3.66E-02
MF	0005125	cytokine activity	*IL33, IL36B, CCL20, CXCL3, CXCL5, PPBP, IL17C*	7.21E-04
MF	0016628	oxidoreductase activity, acting on the CH-CH group of donors, NAD or NADP as acceptor	*AKR1C1, AKR1C2, AKR1C3*	2.66E-03
MF	0016614	oxidoreductase activity, acting on CH-OH group of donors	*AKR1C1, ALDH3A1, ADH7, AKR1B10, AKR1C2, AKR1C3*	4.47E-04
MF	0008106	alcohol dehydrogenase (NADP+) activity	*AKR1C1, ALDH3A1, AKR1B10, AKR1C2, AKR1C3*	6.51E-06
MF	0004033	aldo-keto reductase (NADP) activity	*AKR1C1, ALDH3A1, AKR1B10, AKR1C2, AKR1C3*	7.03E-06
MF	0004032	alditol:NADP+ 1-oxidoreductase activity	*AKR1C1, AKR1B10, AKR1C2, AKR1C3*	7.03E-06
MF	0047834	D-threo-aldose 1-dehydrogenase activity	*AKR1C1, AKR1B10, AKR1C2, AKR1C3*	2.77E-05
MF	0016903	oxidoreductase activity, acting on the aldehyde or oxo group of donors	*ALDH3A1, ADH7, AKR1B10, AKR1C3*	7.14E-04
MF	0008009	chemokine activity	*CCL20, CXCL3, CXCL5, PPBP*	7.76E-04
MF	0018636	phenanthrene 9,10-monooxygenase activity	*AKR1C1, AKR1C2, AKR1C3*	6.51E-06

BP: biological process, CC: Cellular component, MF: Molecular function

(C) Molecular function

The top 20 items of molecular function with which S100A9 affects HNE cells are shown in Figure 21. Analyzing the molecular functions of the top 10 items proved that these are related to enzymes related to oxidoreductase activity, except for 2 items that affect cytokine activity and chemokine activity. These enzymes were *ADH7*, *ALDH3A1*, *AKR1C1*, *AKR1C2*, *AKR1C3*, and *AKR1B10*, all reduced by the stimulation of S100A9.

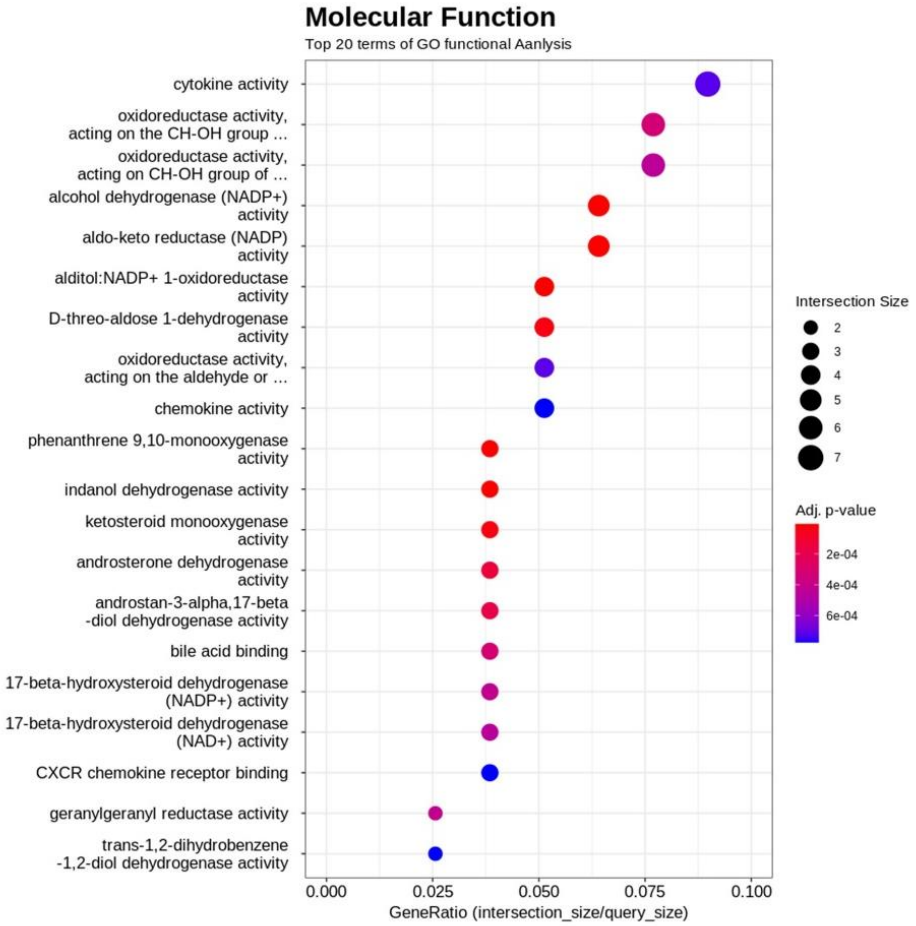

Figure 21. Molecular function in gene ontology for S100A9

These genes also showed a tendency to decrease by S100A8 and calprotectin, similarly to when S100A9 was administered (Table 5). These genes were associated with enzymes involved in the metabolism of retinol to retinaldehyde and retinoic acid[31]. In other words, S100A9 was thought to decrease retinoic acid, which is involved in the proliferation and differentiation of HNE cells, by downregulating *ADH7* and *ALDH3A1* involved in retinoic acid metabolism.

Table 5. Gene ontology group analysis of related genes

Gene	Description	S100A8/control		S100A9/control		Calprotectin/control	
		log_2FC	P-value	log_2FC	P-value	log_2FC	P-value
SPRR2F	small proline rich protein 2F	1.56736	0.27044	2.71980	0.01428	1.44677	0.36561
SPRR2E	small proline rich protein 2E	1.55851	0.00298	2.54834	0.00000	1.26807	0.11248
SPRR2B	small proline rich protein 2B	1.48575	0.00388	2.33178	0.00000	1.24921	0.10532
SPRR2A	small proline rich protein 2A	1.53340	0.00290	2.31414	0.00000	1.27038	0.09609
PI3	peptidase inhibitor 3	1.16446	0.44048	2.01173	0.00041	-1.06028	0.76725
MMP1	matrix metallopeptidase 1	1.81071	0.19440	2.51962	0.04375	1.04498	0.92360
ADH7	alcohol dehydrogenase 7	-2.10562	0.04298	-3.88608	0.00024	-2.04058	0.05303
ALDH3A1	aldehyde dehydrogenase 3 family member A1	-1.74572	0.21023	-3.28206	0.00766	-2.80511	0.02063
AKR1C1	aldo-keto reductase family 1 member C1	-1.88967	0.11547	-2.27118	0.04292	-2.16559	0.05647
AKR1C2	aldo-keto reductase family 1 member C2	-1.53822	0.18735	-2.24952	0.01327	-1.77336	0.08004
AKR1C3	aldo-keto reductase family 1 member C3	-1.66883	0.15616	-2.29460	0.02182	-1.91597	0.07239
AKR1B10	aldo-keto reductase family 1 member B10	-1.40612	0.12168	-2.24331	0.00026	-1.62930	0.02701

IV. DISCUSSION

The purpose of this study was to confirm that S100A8 and S100A9, known as DAMPs, increased in nasal epithelium under inflammatory conditions and to investigate the effects of increased S100A8 and S100A9 on HNE cells. Additionally, in CRS caused by chronic inflammation of the nasal mucosa, we tried to determine whether S100A8 and S100A9 are factors that affect tissue remodeling, such as squamous metaplasia. To confirm this hypothesis, bulk RNA sequencing data was analyzed to determine the effects of S100A8, S100A9, and calprotectin on HNE cells using the HNE cell culture model. In addition, biological processes, cellular compartments, and molecular functions were analyzed through IPA and gene onotology functional analyses, and mechanisms of S100A8, S100A9, and calprotectin on tissue remodeling were investigated. As a result, similarities and differences were confirmed with respect to the effects of S100A8, S100A9, and calprotectin on HNE cells. In particular, we found that increased S100A9 induces the downregulation of *ADH7* and *ALDH3A1* involved in retinoic acid metabolism and reduces retinoic acid production, leading to squamous metaplasia as a result of abnormal HNE cell proliferation and differentiation.

The co-expression of S100A8 and S100A9 was required for stability[32], but they responded differently depending on cell types and stimuli. In macrophages, S100A8 was induced by TLR ligands, such as LPS and poly (I:C)[33], and expressed by TNF-α, TGF-β, and IFN-γ[34]. In microvascular endothelial cells, S100A8 was increased by IL-1β, but not by TNF-α and IFN-γ. On the other hand, S100A9 was increased by IL-1β and TNF-α[35]. In addition, S100A8 and S100A9 was increased in human primary keratinocytes by TNF-α, IL-1β, and IFN-γ[36]. In this study, when HNE cells was treated with LPS, the expression of S100A8 was increased compared to that of S100A9, and S100A8 and S100A9 were increased by TNF-α and IL-1β but not IFN-γ. Similarly, among the IPA results, cytokines such as TNF, IL1B, IL1A, and IL17A were included in the upstream regulator molecule of S100A9. On the other hand, when HNE cell was treated with the anti-inflammatory cytokines IL-4 and IL-13, S100A8 and S100A9 were suppressed. These results showed

similar findings to the decrease of S100A8 and S100A9 when IL-4 and IL-13 were treated in keratinocytes[36], macrophages[33], and microvascular endothelial cells[37].

Tissue remodeling is defined as the reorganization or change of an existing tissue[38]. It is a process of inflammation, an immune response to external substances, and a change in living organisms to adapt to external environments. CRS is a chronic inflammation of the nasal cavity, and tissue remodeling, such as subepithelial fibrosis, goblet cell hyperplasia, basement membrane thickens, and squamous metaplasia is observed[10]. According to a report by Barham et al., tissue remodeling is statistically different for CRSwNP than for CRSsNP. In particular, squamous metaplasia was observed in 23% of CRSwNPs, whereas CRSsNPs were observed in 6% of their cases[14]. In this study, squamous metaplasia was not observed in the healthy and CRSsNP groups, but squamous metaplasia was observed in 50% of CRSwNPs.

The expression of S100A8, S100A9, and calprotectin was confirmed in the epithelial layer through H&E and immunohistochemistry analyses by a pathologist using CRS patient tissue. It was confirmed that S100A8 and S100A9 were more strongly expressed in the squamous epithelium than in the normal nasal epithelium. On the other hand, the expression of calprotectin was not observed in the squamous epithelium, unlike the expression in inflammatory cells. As for the reason why calprotectin expression was different from that of S100A8 or S100A9, additional research is needed to determine whether calprotectin production is due to a structural difference in the heterodimer complex or a function independent of squamous metaplasia. Nevertheless, immunohistochemistry and immunofluorescence were performed using Involucrin, one of the markers of squamous metaplasia, and Involucrin co-localized the expression sites of S100A8 and S100A9. However, it could not be confirmed whether the expression of S100A8 and S100A9 was a result of squamous metaplasia or was caused by squamous metaplasia. When tracheobronchial epithelial cells were induced to undergo squamous metaplasia using retinoic acid deficiency culture media, S100A8 and S100A9 were increased, but the role of S100A8 and S100A9 in squamous metaplasia was unknown[39].

However, the overexpression of S100A8 and S100A9 induced an impair of cell proliferation, survival, and differentiation in HaCaT keratinocytes. In addition, it increased the expression of keratinocyte differentiation markers Involucrin and Filaggrin and was suggested to be involved in tissue remodeling and wound repair[19]. In polyp tissue from CRSwNP, the increased S100A9 expression coincides with elevated MMP production, which is involved in tissue remodeling[22]. Similarly, our results were obtained from conditional experimenting for bulk RNA sequencing. When treated with S100A8 and S100A9, it was found that Involucrin and MMP9 increased, causing tissue remodeling, such as squamous metaplasia.

S100A8 and S100A9 are mostly expressed together due to stability maintenance; their functions are also similar to each other. S100A8 and S100A9 have been reported to be involved in cell proliferation, differentiation, apoptosis, energy metabolism, Ca^{2+} homeostasis, inflammation, and tumor migration/invasion by interacting with various target proteins, including enzymes, transcription factors, receptors, cytoskeletal subunits, and nucleic acids[40]. However, as shown in the bulk RNA sequencing results of this study, the effects of S100A8, S100A9, and calprotectin on HNE cells showed similar trends but functionally different findings. Above all, S100A9 showed a statistically significant effect on HNE cells as opposed to calprotectin and S100A8, which were shown to be involved in IL-17 signaling and the wound healing signal pathway. Recently, Konieczny et al. reported that IL-17 is involved in tissue remodeling[41]. From our experimental results, it appears that the effect of S100A9 on tissue remodeling is related as it is related to S100A9 in the IL-17 pathway and affects the gene involved in tissue remodeling. However, further verification is needed. In addition, S100A8 showed similar findings to S100A9, but above all, it was confirmed that with the stimulation of S100A9, *MMP1* and *MMP10*, tissue remodeling markers, and *SPRR2A*, *SPRR2B*, *SPRR2E*, and *SPRR2F* observed in the squamous epithelium were increased. Through these results, we confirmed the hypothesis that the stimulation of S100A8 and S100A9 induces tissue remodeling, such as squamous metaplasia, in human nasal epithelium.

In the top 10 molecular function analysis performed after HNE cells treatment with S100A9, the remaining 8 functions were related to oxidoreductase activity, alcohol dehydrogenase, and aldo-keto reductase, excluding cytokine activity and chemokine activity related to the IL-17 signaling pathway. Genes related to the eight molecular functions were summarized with *ADH7*, *ALDH3A1*, *AKR1C1*, *AKR1C2*, *AKR1C3*, and *AKR1B10*, which were classified as alcohol dehydrogenase, aldehyde dehydrogenase, and aldo-keto reductase. Gallego et al. found that alcohol dehydrogenase, aldehyde dehydrogenase, and aldo-keto reductase catalyze retinoic acid biosynthesis when retinol is oxidized to retinaldehyde and retinaldehyde is oxidized to retinoic acid[31]. In particular, retinoic acid, an active metabolite of retinol (vitamin A), is an essential substance for normal cell proliferation and differentiation in HNE cells, and there are many reports that squamous metaplasia progresses when cell culture is performed without retinoic acid[28,39,42]. Therefore, this study proposes that increased S100A8 and S100A9 due to inflammation are modulated enzymes involved in retinoic acid metabolism, leading to the depletion of retinoic acid and induction of squamous metaplasia.

This study aimed to prove that S100A8 and S100A9 in HNE cells are increased by inflammation and are involved in tissue remodeling, especially squamous metaplasia, as a pro-inflammatory function. However, this study had some limitations. First, molecular function results obtained through bulk RNA sequencing data suggested that S100A8 and S100A9 are involved in retinoid acid metabolism, but further verification was not made on this; thus, further research is needed. Clinically, since the nasal polyps of patients with CRSwNP have a different tissue from the ethmoid mucosa, careful attention is required when classifying the participant groups. In addition, additional research is needed for functional studies through the knock-down of S100A8 or S100A9. Nevertheless, it is a novel finding to suggest for the first time that S100A8 and S100A9 are involved in tissue remodeling, such as squamous metaplasia, by downregulating retinoic acid metabolism in HNE cells.

V. CONCLUSION

The summary of this study is shown in Figure 22. The increase of S100A8 and S100A9 in HNE cells was induced by pro-inflammatory cytokines and inhibited by anti-inflammatory cytokines. Increased S100A8 and S100A9 were involved in reducing retinoid acid production by downregulating retinoic acid metabolism. As a result of abnormal cell proliferation, tissue remodeling and squamous metaplasia were induced. Clinically, increased S100A8 and S100A9 in CRS tissue can be considered as a biomarker that reflects the severity of CRS.

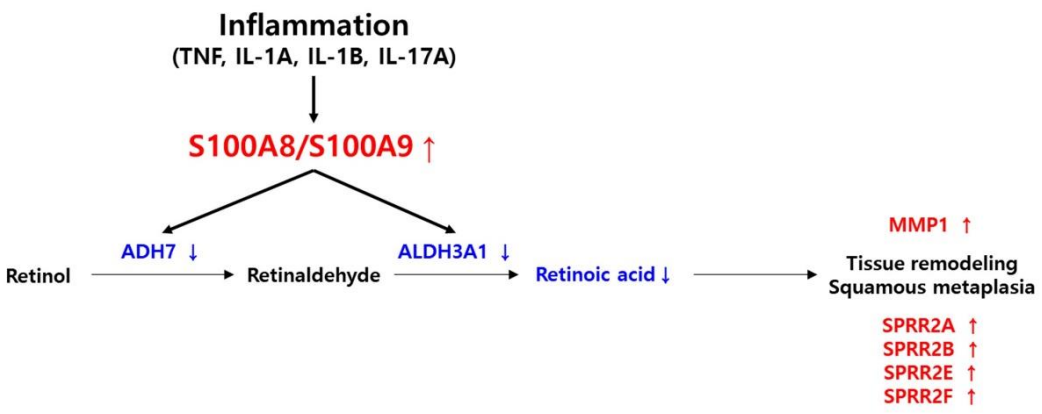

Figure 22. Summary of the study

Chapter II.

Calprotectin is involved in eosinophil extracellular traps in chronic rhinosinusitis.

I. INTRODUCTION

Calprotectin is a heterodimeric complex of S100A8 and S100A9 and one of the most well-known antimicrobial peptides. Calprotectin has an important role in the innate immune response by protecting the host against infection and performing pro-inflammatory functions[43]. The origins of calprotectin are expressed mostly in myeloid cells, such as neutrophils[44] and monocytes[45]. Extracellular secretion of calprotectin is caused by cell destruction and programmed cell death[46], but an inflammatory signal reaction also prompts its translocation from the cytoplasm to the cell surface[47]. The antibacterial effect of calprotectin functions by interfering with bacterial survival by chelating essential metals, such as Zn^{2+}, Mn^{2+}, and Fe^{2+} [48-50]. Specifically, to defend the host from infection, neutrophils kill microorganisms intracellularly by phagocytosis or in the extracellular space by the release of neutrophil extracellular traps (NETs) which block the spread of pathogens by degranulation of antimicrobial proteins including calprotectin[51].

In the upper respiratory tract, chronic rhinosinusitis (CRS) is characterized by chronic inflammation of paranasal sinuses. The phenotype of CRS is divided into chronic rhinosinusitis with nasal polyps (CRSwNP) and chronic rhinosinusitis without nasal polyps (CRSsNP) depending on the nasal polyp visualized on the endoscope[24] Recently, endotypes of CRS have been classified into types 1, 2, and 3 according to molecular biomarkers[52]. In particular, eosinophils in tissue are a marker that reflects the disease severity of CRS, which is classified into eosinophilic CRS (ECRS) and non-eosinophilic CRS (NCRS) according to the degree of eosinophils infiltration, but eosinophils are observed predominantly in CRSwNP[24].

As with tissue eosinophils in CRS, a recent study has suggested that serum calprotectin could be a disease severity biomarker for CRS[53]. Tissue expression of calprotectin was higher in patients with CRSwNP than in healthy controls and patients with CRSsNP, and was associated with host defense mechanisms against infection by forming NETs with neutrophil-secreted calprotectin[20,23]. However, CRSwNP is considered a chronic

inflammatory disease characterized by type 2 inflammation, similar to asthma, and is closely related to eosinophils[54,55]. Similar to neutrophils, eosinophils, which are related to helminthic infections and allergic responses, form extracellular traps as an innate immune response to viral and/or bacterial infection, which is called eosinophilic extracellular traps (EETs)[56]. Furthermore, Ueki et al proposed that EETs are important for CRSwNP development[57].

Although, previous studies have explored S100A8 and S100A9 expression in eosinophils[58,59], but no studies have investigated the relationship between calprotectin and eosinophils in CRS. Therefore, we investigated the relationship between calprotectin and eosinophils using tissues from patients with CRSwNP to establish calprotectin's involvement in EETs. In addition, we investigated associations between calprotectin and clinical findings to evaluate its suitability as a CRS severity biomarker.

II. MATERIALS AND METHODS

1. ECRS in vivo mouse model

We used the ECRS mouse model previously established by our group[60] to perform an *in vivo* experiment investigating the relationship between calprotectin and eosinophils and neutrophils. Six-week-old C57BL/6N female mice were purchased from Orient Bio (Seongnam, Korea) and maintained under specific pathogen-free conditions. The control group (n = 2) was treated with phosphate-buffered saline (PBS), and the ECRS group (n = 2) was intranasally administered four multiple-allergen mixtures for 12 weeks. The multiple-allergen mixture included 20 μg of house dust mite extract (*Dermatophagoides pteronyssinus*; Greer Laboratories, Lenoir, NC, USA), 20 μg of *Aspergillus fumigatus* (Greer Laboratories), 20 μg of *Alternaria alternata* (Greer Laboratories), and 1 μg of *Staphylococcus aureus* protease (Abnova, Taipei) dissolved in sterile PBS. In total, 30 μl was injected into both nostrils (15 μl per nostril). All mice were sacrificed 24 hours after the last treatment at 12 weeks.

2. Participants

The appropriate institutional review board and ethics committee (No. 2020-05-004) reviewed and approved this study. All subjects provided written informed consent before enrolment. Furthermore, we performed all procedures, including human participants, following the ethical standards of the institutional and national research committee and the 1964 Declaration of Helsinki and its later amendments or comparable ethical standards.

The control group included patients (>19 years) with a mucocele or retention cyst at the maxillary sinus requiring a middle meatal antrostomy. Computed tomography (CT) images and surgical findings confirmed that the ethmoid sinus was lesion-free, and the ethmoid mucosa was harvested. On the other hand, CRS was diagnosed and classified based on the 2020 European position paper on rhinosinusitis and nasal polyps[24]. We obtained ethmoid mucosa from CRSsNP patients and nasal polyps from CRSwNP

patients over 19 years old who needed endoscopic sinus surgery because the lesion did not improve after medical treatment. None of the patients had been on an intranasal or oral steroids regimen for at least one month before surgery. Patients with pregnancy, malignancy, chronic disease, or immune deficiency were excluded.

We classified patients with CRS as ECRS or NCRS based on the Japanese Epidemiological Survey of Refractory Eosinophilic Chronic Rhinosinusitis (JESREC) score[61]. The JESREC score is the sum of the scores for each item based on the following criteria: 1) disease side (one side: 0 vs both sides: 3), 2) nasal polyps (absent: 0 vs present: 2), 3) an ethmoid sinus shadow on CT (negative: 0 vs positive: 2), and 4) the percentage of eosinophils in the blood (less than 2 %: 0, 2 %< value ≤5 %: 4, 5 %< value ≤10 %: 8, and more than 10 %: 10). A JESREC score of 11 or higher was classified as ECRS, and a score of less than 11 was classified as NCRS. CRS disease severity was based on Lund-Mackay CT scores[25], a well-known method that calculates scores for each side of the nose based on CT findings and combines the two scores to obtain the final score. Olfactory function was measured using the YSK olfactory function test Kit (YOF test; Kimex Co., Suwon, Korea) before surgery, and the threshold, discrimination, and identification scores were measured as previously reported[26]. The sum of these three scores was defined as the olfactory function score. Finally, we collected demographic data, including age, sex, underlying diseases (e.g., allergies and asthma), the sino-nasal outcome test 22 score and blood tests (e.g., white blood cell count and neutrophil and eosinophil percentages).

3. Histopathological assessment

Ethmoid mucosa and nasal polyp tissue excised from the patients were fixed with 10 % formalin for at least 24 hours. The mouse heads were fixed in 4 % paraformaldehyde and then decalcified in 10 % ethylenediaminetetraacetic acid for two weeks. All fixed tissues were embedded in paraffin. Each paraffin block was sliced into 4-μm-thick sections. Sliced specimens were prepared for histological analysis with haematoxylin and eosin

staining. Tissue eosinophils were counted by a pathologist in ten random high-power fields (HPF; 400×) using an Olympus U-TV0.63XC optical microscope following a previously described method[62], and the average values were used for analyses.

4. Immunohistochemistry

Immunohistochemistry was performed using BenchMark ULTRA automated slide stainer combined with VENTANA detection kits (Ventana Medical Systems, Tucson, AZ, USA) following the manufacturer's protocol. After deparaffinisation, the slides were treated using the peroxidase inhibitor included in the detection kit for 4 min at room temperature without antigen retrieval to inhibit endogenous peroxidase. The first antibody reaction was incubated for 28 min at 36 °C with a mouse monoclonal anti-calprotectin antibody (1:100, ab17050, Abcam, Cambridge, UK). The negative control was incubated with nonimmune serum instead of the primary antibody. Next, the sections were incubated in the OptiView DAB IHC Detection Kit solution (Ventana Medical Systems) for 8 min. Counterstaining and post-counterstain were performed for 4 min using haematoxylin and bluing reagent. As previously reported definitions of extracellular traps (ETs)[63]. using immunohistochemical images for calprotectin, ETs were defined as calprotectin showing spider's web-like structures in extracellular lesions without being localized within cells. Calprotectin-positive cells were counted in ten random HPFs (400×), the average values were used for analyses, which was performed with Image J software (version 1.53a; National Institutes of Health, Bethesda, MD, USA).

5. Immunofluorescence

Neutrophils secrete calprotectin. Thus, immunofluorescence was performed using eosinophil and neutrophil markers to confirm the origin of calprotectin. Paraffin-embedded tissue slides were deparaffinised and rehydrated. After antigen retrieval, the tissue sections were blocked for one hour at room temperature using 5 % bovine serum albumin. The primary antibody reaction was incubated overnight at 4 °C in

a humidified chamber. The primary antibodies were a mouse monoclonal anti-calprotectin antibody (1:500, ab17050, Abcam), a rabbit polyclonal anti-eosinophil major basic protein (MBP) antibody (1:500, PA5-102628, Invitrogen, Carlsbad, CA, USA) and a goat polyclonal anti-myeloperoxidase (MPO) antibody (1:200, AF3667, R&D Systems, Minneapolis, MN, USA) for triple labelling. A mouse monoclonal anti-calprotectin antibody (1:250, MA1-33972, Invitrogen) was used as the primary antibody for calprotectin in mouse tissue. Afterwards, the secondary antibody reaction was incubated at the room temperature for 30 min using Alexa Fluor 488 goat anti-Mouse immunoglobin (Ig) G polyclonal secondary antibody (1:1000, A11001, Invitrogen), Alexa Fluor 568 goat anti-Rabbit IgG polyclonal secondary antibody (1:1000, A11011, Invitrogen) and Alexa Fluor Plus 647 donkey anti-Goat IgG polyclonal secondary antibody (1:1000, A32849, Invitrogen). All negative controls were immunostained with nonimmune serum instead of primary antibodies. Nucleic acids were stained with 4′,6-diamidino-2-phenylindole (i.e., DAPI, Invitrogen). Finally, coverslips were mounted onto the slides with fluorescent mounting media (DAKO, Glostrup, Denmark).

NETs and EETs were defined and detected as morphologic changes as previously described[56,62,64]. First, the nucleus was confirmed using DAPI. The nucleus of the non-ETosis granulocytes showed a typically intact lobulated morphology with clear separation of euchromatin and heterochromatin, whereas the nucleus of ETs showed loss of lobulation and diffused DAPI staining due to decondensed chromatin. Simultaneously, MPO, a neutrophil azurophilic granule, or MBP, an eosinophil-specific granule protein, was scattered around the nucleus without compartmentalization within the cell. If calprotectin matched MPO, it was considered to be expressed on NETS, whereas if it co-localized with MBP, it was considered to be expressed on EET. Fluorescence images were obtained with a Zeiss LSM 700 confocal laser scanning microscope (Carl Zeiss, Berlin, Germany) and analysed using ZEISS ZEN 3.2 blue edition (Carl Zeiss, Jena, Germany).

6. Statistical analyses

All statistical analyses were performed using SPSS Statistics 26.0 (IBM Corp., Armonk, NY, USA). Comparisons among the three groups were performed by one-way analysis of variance, and the differences between the two groups were compared by two-sample t-tests. Continuous data are presented as means ± standard deviations. Finally, we analysed correlations between calprotectin and the clinical variables using Pearson's correlation coefficient. A p-value of <0.05 was considered statistically significant.

III. RESULTS

1. Calprotectin, eosinophils and neutrophils in ECRS mice

We performed immunofluorescence using three primary antibodies simultaneously to evaluate the relationships among calprotectin, eosinophils and neutrophils in ECRS mice. Calprotectin expression was consistent with MBP expression, a known eosinophil marker (Figure 23 A). In addition, the ECRS mice had significantly more calprotectin (Cal+), eosinophil and neutrophil positive cells than the control mice (Figure 23B). The ECRS mice also had more MBP and MPO-positive cells (MBP+ and MPO+, respectively) than the control mice. Therefore, in type 2 dominant inflammation such as ECRS, neutrophils and eosinophils express calprotectin, confirming its involvement in innate immunity.

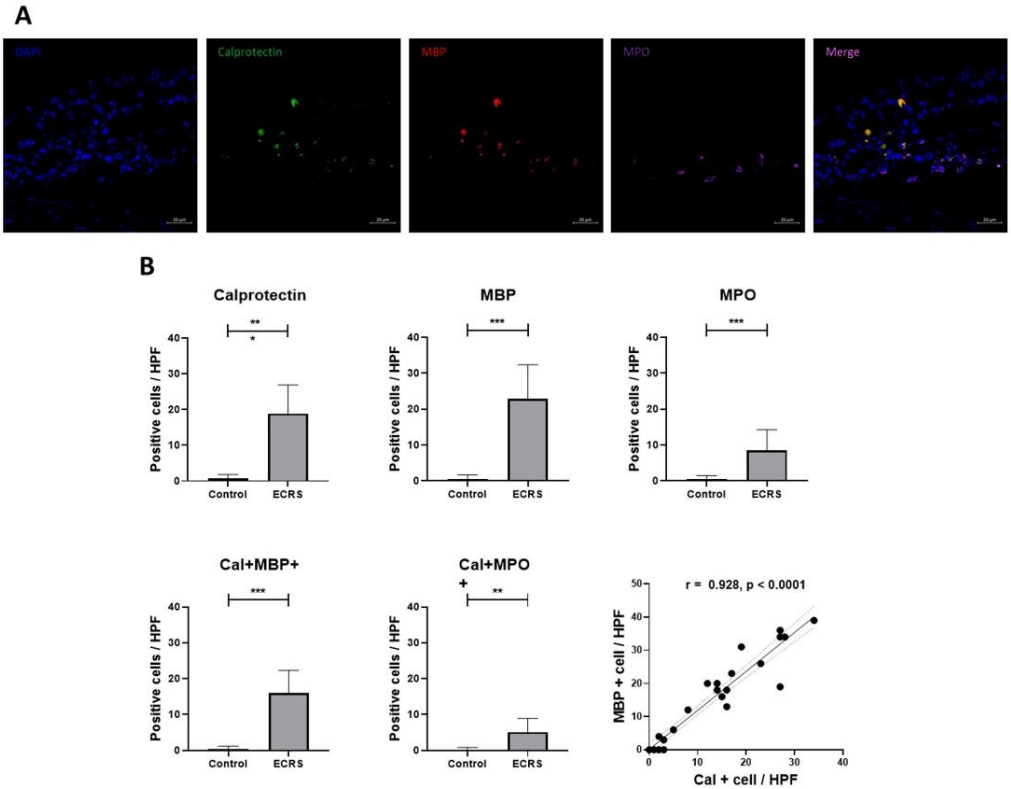

Figure 23. Triple immunofluorescence staining for calprotectin, major basic protein (MBP), and myeloperoxidase (MPO) in the eosinophilic chronic rhinosinusitis (ECRS) mouse model.

(A) Eosinophils (MBP; red), neutrophils (MPO; purple) and calprotectin (green), and calprotectin co-localization with MBP (merge; pink). Control cells stain with 4′,6-diamidino-2-phenylindole (i.e., DAPI, blue). (B) ECRS mice with high calprotectin (Cal+), MBP (MBP+), and MPO (MPO+) positive cells than the control group. ECRS mice with an increase in CAL+MBP+ and CAL+MPO+ cells than the control group, and calprotectin positively correlates with eosinophils. Abbreviations: HPF, high-performance field.
** $p < 0.01$; *** $p < 0.001$.

2. Calprotectin increases proportionally with eosinophils in human tissue

We analysed tissue samples and clinical information collected from 63 patients with ECRS and NCRS to evaluate calprotectin in patients with CRS; Table 1 presents their demographic data. The eosinophil count was significantly higher in the ECRS group than in the NCRS group (22.3 ± 9.4 vs 3.3 ± 2.2, $p < 0.001$; Figure 24A). When classified by phenotype, the CRSsNP and CRSwNP groups did not differ (12.9 ± 11.6 vs 15.5 ± 12.2, $p = 0.48$). However, the CRSwNP group had significantly more Cal+ cells than the control or CRSsNP groups (Figure 24B). Furthermore, the ECRS group had more Cal+ cells than the NCRS group (Figure 24C). Finally, eosinophil-positive and Cal+ cells positively correlated ($r = 0.571$, $p < 0.0001$; Figure 24D). Therefore, the secretion of calprotectin from only neutrophils has limitations in explaining the pathophysiology of CRSwNP, and the secretion of calprotectin from eosinophils could be considered.

Table 6. Participant demographics

	Control	CRSsNP		CRSwNP	
		NCRS	ECRS	NCRS	ECRS
	(n = 10)	(n = 13)	(n = 11)	(n = 10)	(n = 19)
Age, years	58.3 ± 16.1	51.5 ± 13.4	53.3 ± 11.7	49.0 ± 12.7	47.2 ± 15.0
Gender, Female/Male	8/2	1/11	3/8	3/7	4/15
Asthma+, n	0	1	2	0	6
Allergy+, n	2	8	3	5	13
Olfactory function score	25.5 ± 4.0	23.7 ± 5.4	22.0 ± 3.3	27.0 ± 6.2	16.1 ± 8.4
SNOT 22	30.1 ± 14.5	36.5 ± 22.6	33.2 ± 18.4	41.9 ± 18.0	40.6 ± 22.7
Lund-Mackay CT score	2.3 ± 1.6	8.8 ± 4.5	12.3 ± 3.9	10.6 ± 5.6	14.5 ± 6.1
JESREC score	2.6 ± 1.8	5.5 ± 2.7	11.9 ± 1.6	6.2 ± 1.8	14.0 ± 2.2
WBC, $10^3/mm^3$	6.5 ± 1.3	6.3 ± 1.4	5.8 ± 0.8	6.6 ± 1.6	6.7 ± 1.3
Neutrophil in blood, %	53.2 ± 10.3	55.9 ± 9.5	55.9 ± 6.8	58.2 ± 10.0	54.4 ± 7.9
Eosinophil in blood, %	2.6 ± 1.8	2.3 ± 1.5	4.0 ± 2.2	1.9 ± 1.0	6.4 ± 2.5
Total IgE, IU/L	127.3 ± 155.6	235.1 ± 276.5	130.4 ± 234.8	247.8 ± 305.8	256.0 ± 211.2

Abbreviations: CRSsNP; chronic rhinosinusitis without nasal polyp, CRSwNP; chronic rhinosinusitis with nasal polyp, NCRS; non-eosinophilic chronic rhinosinusitis, ECRS; eosinophilic chronic rhinosinusitis, SNOT; sino-nasal outcome test, JESREC; Japanese Epidemiological Survey of Refractory Eosinophilic Chronic Rhinosinusitis, WBC; white blood cell; IgE, immunoglobin E.

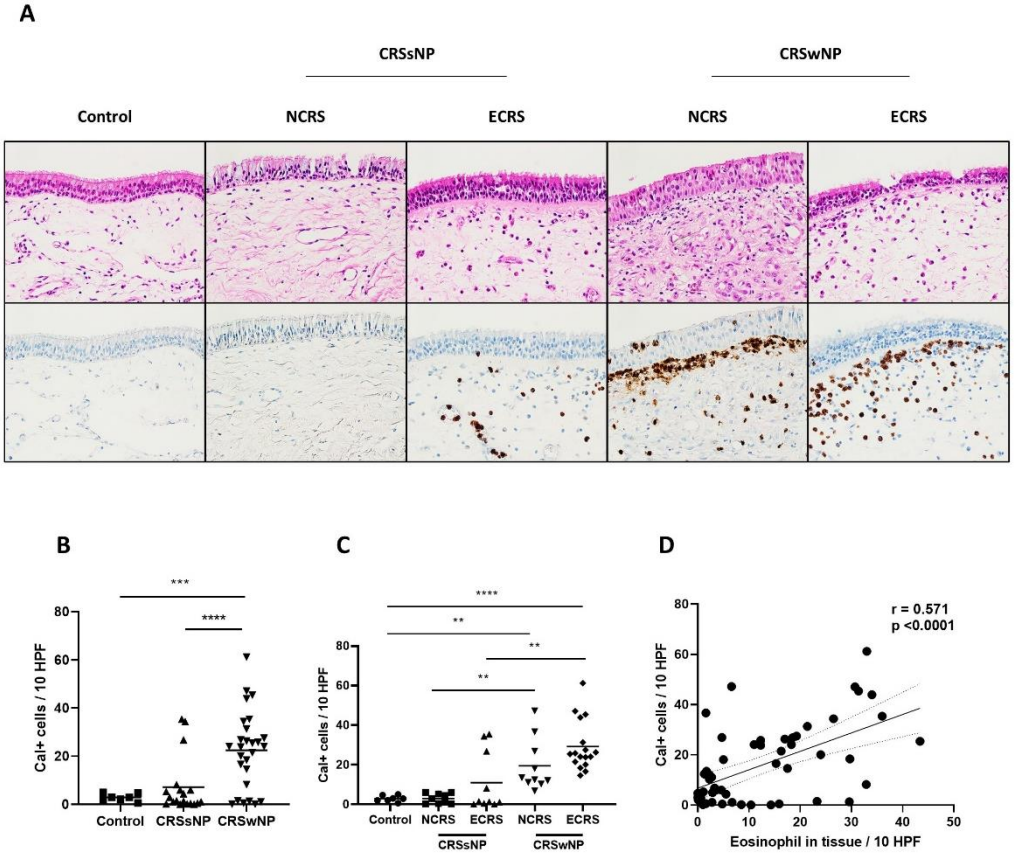

Figure 24. Haematoxylin and eosin and immunohistochemistry staining for calprotectin in human tissue. (A) Eosinophils increase (cells stained in intense pink) in the eosinophilic chronic rhinosinusitis (ECRS) tissues than in the non-eosinophilic chronic rhinosinusitis (NCRS) or control tissues. (B) Calprotectin-positive (Cal+) cells in chronic rhinosinusitis with polyps (CRSwNP) tissue. (C) Calprotectin expression is similar in NCRS and ECRS tissues. (D) The number of Cal+ cells increase proportionally to the number of eosinophils in the tissue.
Abbreviations: CRSsNP, chronic rhinosinusitis without nasal polyp; HPF, high-performance field.
** $p < 0.01$; *** $p < 0.001$; **** $p < 0.0001$.

3. Calprotectin originates from neutrophils and eosinophils

We evaluated the origin of calprotectin using MPO (a neutrophil marker) and MBP (an

eosinophil marker). MPO+ and MPB+ cells were consistent with Cal+ cells (Figure 25A). The MPO+Cal+ cells to total Cal+ cells ratio did not differ between the NCRS and ECRS groups, statistically, but the NCRS group had more MPO+Cal+ cells than the ECRS group (Figure 25B). The MBP+Cal+ cells to total Cal+ cells ratio was significantly higher in the ECRS group than in the NCRS group (Figure 25C). These results indicate that both neutrophils and eosinophils secrete calprotectin.

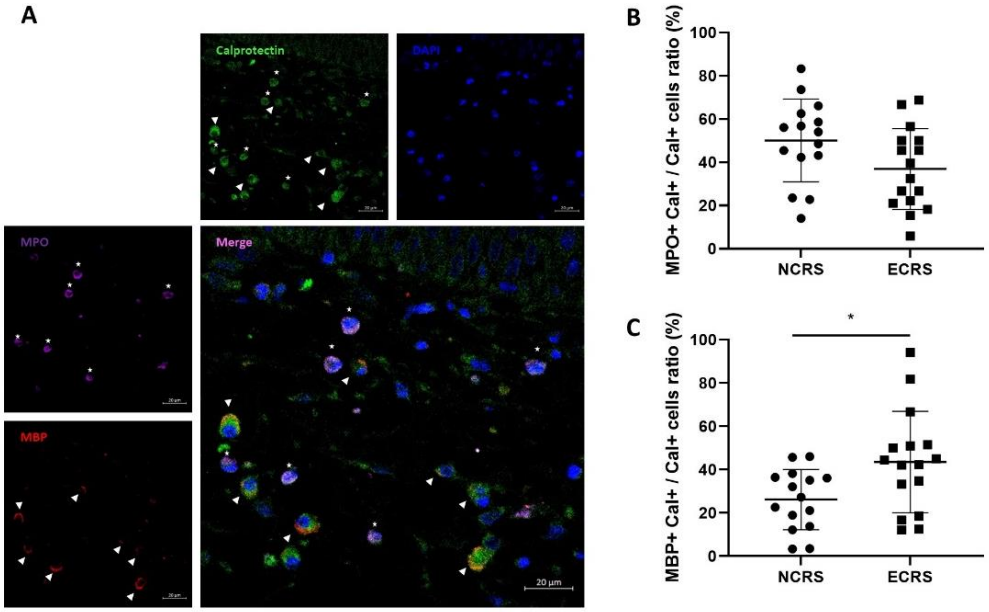

Figure 25. Triple immunofluorescence staining for calprotectin, major basic protein (MBP), and myeloperoxidase (MPO) in human tissue. (A) Calprotectin staining (green) is consistent with MPO (purple) and MBP (red) staining. Stars: cells with overlapping calprotectin and MPO staining. Arrowheads: cells with overlapping calprotectin and MBP staining. (B) Non-eosinophilic chronic rhinosinusitis (NCRS) tissues with an increase in MPO (MPO+) and calprotectin (Cal+) positive cells than eosinophilic chronic rhinosinusitis (ECRS) tissues. (C) The MBP+Cal+ cells to total Cal+ cells ratio is higher in ECRS tissues than in NCRS tissues.
* $p < 0.01$.

4. ETTs contain calprotectin

We analysed the immunohistochemistry of calprotectin in patient tissues to determine the relationship between calprotectin and ETs. Cal+ cells with ETs were primarily observed in the submucosal layer bordering the basal cells rather than the epithelial layer (Figure 26A). In addition, calprotectin containing ETs that formed a web were more prominent in polyp tissues than ethmoid tissues regardless of ECRS or NCRS (Figure 26B, 26C). As the number of Cal+ cells increased, the number of calprotectin containing ETs also increased (Figure 26D). However, the immune cells responsible for calprotectin could not be identified. Immunofluorescence of calprotectin, MPO and MBP confirmed calprotectin's involvement in NETs, which was more prominent in the NCRS group than in the ECRS group (Figure 26E, 26F). In addition, we confirmed that calprotectin was contained in EETs (Figure 26G). However, the number of EETs with calprotectin was more pronounced in ECRS than in NCRS polyps (Figure 26H). Therefore, we confirmed calprotectin (an antimicrobial peptide in CRSwNP) expression in EETs and NETs.

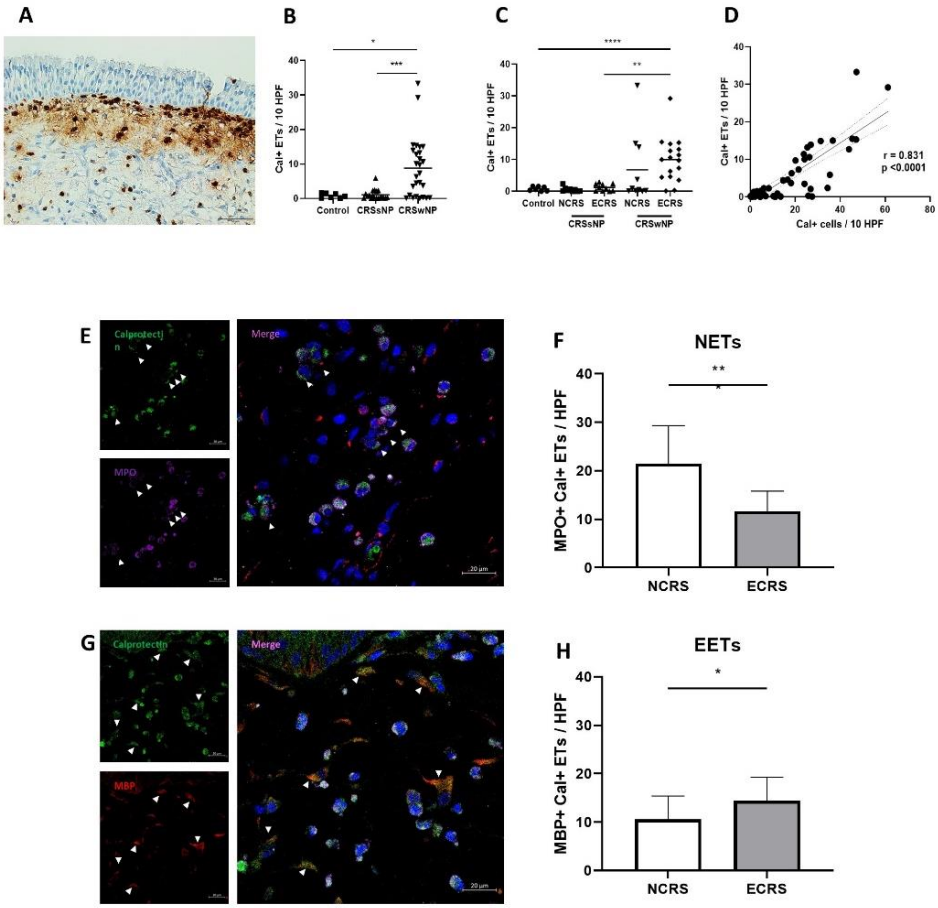

Figure 26. Immunohistochemistry with human tissue. (A) Calprotectin staining with spider web formations, such as extracellular traps (ETs). (B) Chronic rhinosinusitis with polyps (CRSwNP) tissue with an increase in calprotectin positive (Cal+) cells with ETs than chronic rhinosinusitis without nasal polyp (CRSsNP) tissue. (C) ETs comparatively increase in CRSwNP tissue than in control or CRSsNP tissue. (D) The number of ETs increases proportionally to the number of Cal+ cells. Calprotectin expression in neutrophil extracellular traps (NETs) and eosinophil extracellular traps (EETs) by immunofluorescence staining in human nasal polyps. (E) Calprotectin (green; Cal+) and MPO (purple; MPO+)-positive cells co-localize as a NETs. (Arrowhead: corresponding calprotectin in neutrophil.) (F) Non-eosinophilic chronic rhinosinusitis (NCRS) tissue with an increase in NETs calprotectin than eosinophilic chronic rhinosinusitis (ECRS) tissue.

(G) MBP (red; MBP+)-positive cells with EETs were consistent with Cal+ (green) cells. (Arrowhead: calprotectin co-localizes in eosinophil.) (H) ECRS tissue with higher EETs calprotectin than NCRS tissue.

Abbreviations: ECRS, eosinophilic chronic rhinosinusitis; HPF, high-performance field; NCRS, non-eosinophilic chronic rhinosinusitis.

* $p < 0.05$; ** $p < 0.01$; *** $p < 0.001$; **** $p < 0.0001$.

5. Calprotectin in tissue reflects CRS severity

We explored various correlations with clinical findings to determine whether calprotectin expressed in tissue reflects CRS disease severity. First, as the number of Cal+ cells in the tissue increased, the olfactory function decreased ($r = -0.403$, $p = 0.005$; Figure 27A). Furthermore, the Lund-Mackay CT score, reflecting CRS disease severity, positively correlated with the number of Cal+ cells in the tissue ($r = 0.426$, $p = 0.001$; Figure 27B). In addition, as the number of Cal+ cells increased the JESREC score ($r = 0.541$, $p < 0.001$; Figure 27C) and the number of eosinophils in the blood increased ($r = 0.668$, $p < 0.001$; Figure 27D). These results suggest that calprotectin can be a CRS disease severity biomarker.

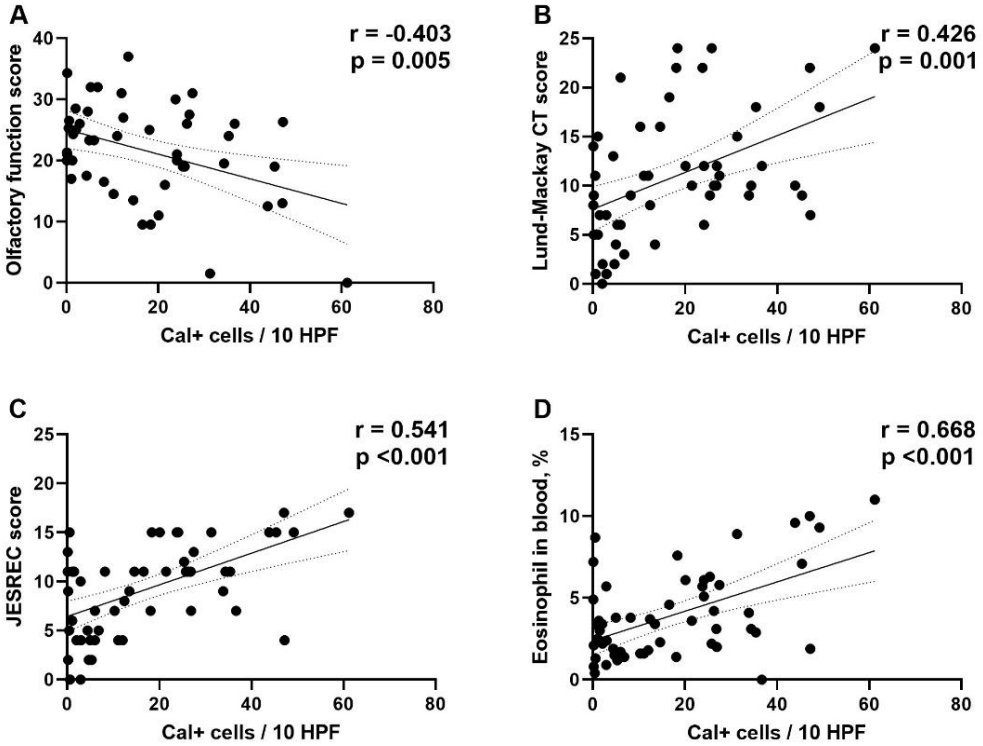

Figure 27. Correlations between calprotectin-positive (Cal+) cells in tissues and clinical findings. (A) The olfactory function scores. (B) The Lund-Mackay computed tomography (CT) score. (C) The Japanese Epidemiological Survey of Refractory Eosinophilic Chronic Rhinosinusitis (JESREC) score. (D) The blood eosinophil level.

Abbreviations: HPF, high-performance field.

IV. DISCUSSION

Inflammation is a host defense mechanism against noxious stimuli (e.g., pathogens or irritants[65]), and inflammatory cells (e.g., neutrophils, eosinophils, and mast cells) play a significant role in disease pathophysiology. Calprotectin is vital in inflammation development and is secreted by various cells, including myeloid cells (e.g., neutrophils[44] or monocytes[45]) and bronchial epithelial cells[66]. However, neutrophils are the most common cell to secrete calprotectin (up to 60%). Therefore, various inflammatory diseases, such as inflammatory bowel disease[67], rheumatoid arthritis[68], psoriasis[69], asthma[70,71], and coronavirus 2019[72], are associated with calprotectin and neutrophils. Previous CRS studies reported that calprotectin increased in patients with CRSwNP compared to patients with CRSsNP and healthy controls. Furthermore, this result correlated with neutrophils using neutrophil-specific markers, such as MPO and neutrophil elastase[20,23].

Although CRS is traditionally phenotyped into CRSwNP and CRSsNP according to the presence or absence of nasal polyps[24], the phenotype of CRS did not directly relate to the pathophysiologic diversity of CRS patients[73]. In addition, along with recent advanced technologies in molecular immunity, CRS patients can be classified into three main endotypes— type 1, 2, and 3 based on specific mechanisms or molecular biomarkers[52]. However, CRSwNP is classified as a type 2 inflammatory disease involving tissue eosinophilia, and eosinophils play an essential role in the pathogenesis[54,55]. Nevertheless, Delemarre et al. reported that neutrophilic inflammation was observed in CRSwNP[74]. Furthermore, they noted that in patients with severe and uncontrolled CRSwNP, eosinophils and neutrophils may be essential for the maintenance of disease chronicity due to mixed eosinophilic-neutrophilic inflammation caused by interactions rather than separate processes[75]. Similarly, Poposki et al also claimed the findings of increased neutrophils in eosinophilic CRSwNP, and mentioned the association with the recurrence of nasal polyp[76]. From the perspective of mixed eosinophilic-neutrophilic inflammation, this study focused on the hypothesis that calprotectin, known as an antimicrobial protein,

might also be expressed in eosinophils, deviating from the conventional view that it is expressed in neutrophils. Consequently, we demonstrated that neutrophils and eosinophils express calprotectin. Furthermore, we confirmed that calprotectin was involved in EETs as a host defense mechanism and expression of calprotectin in CRS tissue could serve as a biomarker that better reflects CRS severity.

In this study, for the first time, we confirmed the relationship between eosinophils and calprotectin in CRS tissues. Moreover, to confirm the relationship between calprotectin, eosinophils and neutrophils, we performed triple immunofluorescence using antibodies against eosinophils (MBP) and neutrophils (MPO) to identify cells secreting calprotectin. As a result, we identified eosinophils, neutrophils and calprotectin in CRS tissues, confirming that neutrophils and eosinophils secreted calprotectin.

We also identified a significant difference in the number of Cal+ cells between CRSwNP tissues and CRSsNP and control tissues, consistent with previous reports of increased calprotectin in patients with CRSwNP[20,23]. Furthermore, we classified CRS patients into NCRS and ECRS groups based on their JESREC score, finding more calprotectin in the ECRS group, which positively correlated with eosinophil count. This result verifies the relationship between calprotectin and eosinophils and confirms that neutrophils and eosinophils secrete calprotectin.

When tissue is infected with bacteria, calprotectin secreted into the extracellular space from neutrophils, macrophages, and monocyte induce an inflammatory reaction from inflammatory cytokines[77]. Calprotectin is also secreted after tissue damage, cellular necrosis[46] and NETs[51]. Phagocytosis and degranulation proceed through NETs formations, and calprotectin (an antimicrobial protein) is secreted[78]; these processes are established pathophysiologic mechanisms of CRS. In this study, we confirmed NETs and EETs in the tissue via immunofluorescence based on their published definitions[62]. Consequently, we determined that calprotectin is involved in the innate immune response through EETs, similar to NETs.

Eosinophilia in CRS patients strongly correlates with the type 2 inflammatory response

and is associated with a high CRS recurrence rate and incidence and severity of asthma[54]. Clinically, ECRS patients have poor olfactory function than NCRS patients[79], and EETs in the tissues of patients with CRS positively correlate with clinical severity[80]. In this study, as the number of Cal+ cells increased, the olfactory function decreased, but the Lund-Mackay CT and JESREC scores, reflecting CRS severity, increased. These results are similar to recent reports identifying a correlation between serum calprotectin and symptom severity in patients with CRS[53]. In addition, the tissue and blood eosinophil levels positively correlated with calprotectin positive cells. These results suggest that since calprotectin is expressed not only in neutrophils but also in eosinophils, the fact that the expression of calprotectin in tissues is correlated with the clinical findings of CRS patients may include the previous results that increased tissue eosinophils reflect the CRS severity. Therefore, tissue calprotectin expression may be an appropriate biomarker reflecting CRS severity, as it is expressed in inflammatory cells such as neutrophils and eosinophils.

Overall, neutrophils and eosinophils express calprotectin in patients with CRS. Although the calprotectin expression ratio in neutrophils and eosinophils differs based on the CRS subtype, calprotectin as an antimicrobial peptide may involve in EETs, similar to NETs. These results suggest that calprotectin level is increased regardless of the neutrophil or eosinophil level in type 2 inflammatory conditions, such as CRSwNP. Therefore, the calprotectin expression in CRS tissue can be a disease severity biomarker.

In this study, we demonstrated the relationship between calprotectin and eosinophils using CRS tissue. Nevertheless, the co-localized data of calprotectin and eosinophil markers cannot conclusively demonstrate that eosinophils produce calprotectin. Further experiments to confirm calprotectin expression and EETS using tissue-isolated eosinophils or purified eosinophils are required to show clarity on the relationship between eosinophils and calprotectin. However, the expression of calprotectin in CRS and simultaneously the relationship between calprotectin and inflammatory cells such as eosinophils and neutrophils are demonstrated for the first time.

V. Conclusion

We present the first evidence that neutrophils and eosinophils in CRS tissues express calprotectin. In addition, calprotectin, which is involved in EETs, may play an important role in the innate immune response of CRS. Finally, the expression of calprotectin in the tissues of CRS patients was validated as disease severity biomarker.

REFFERENCE

1. Müller L, Brighton LE, Carson JL, Fischer WA, 2nd, Jaspers I. Culturing of human nasal epithelial cells at the air liquid interface. J Vis Exp 2013; doi:10.3791/50646.
2. Vareille M, Kieninger E, Edwards MR, Regamey N. The airway epithelium: soldier in the fight against respiratory viruses. Clin Microbiol Rev 2011;24:210-29.
3. Zhang N, Van Crombruggen K, Gevaert E, Bachert C. Barrier function of the nasal mucosa in health and type-2 biased airway diseases. Allergy 2016;71:295-307.
4. Müller L, Jaspers I. Epithelial cells, the "switchboard" of respiratory immune defense responses: effects of air pollutants. Swiss Med Wkly 2012;142:w13653.
5. Chen L, Deng H, Cui H, Fang J, Zuo Z, Deng J, et al. Inflammatory responses and inflammation-associated diseases in organs. Oncotarget 2018;9:7204-18.
6. Feghali CA, Wright TM. Cytokines in acute and chronic inflammation. Front Biosci 1997;2:d12-26.
7. Roh JS, Sohn DH. Damage-Associated Molecular Patterns in Inflammatory Diseases. Immune Netw 2018;18:e27.
8. Giroux V, Rustgi AK. Metaplasia: tissue injury adaptation and a precursor to the dysplasia-cancer sequence. Nat Rev Cancer 2017;17:594-604.
9. Bassiouni A, Chen PG, Wormald PJ. Mucosal remodeling and reversibility in chronic rhinosinusitis. Curr Opin Allergy Clin Immunol 2013;13:4-12.
10. Kao SS, Bassiouni A, Ramezanpour M, Finnie J, Chegeni N, Colella AD, et al. Proteomic analysis of nasal mucus samples of healthy patients and patients with chronic rhinosinusitis. J Allergy Clin Immunol 2021;147:168-78.
11. Mynatt RG, Do J, Janney C, Sindwani R. Squamous metaplasia and chronic rhinosinusitis: a clinicopathological study. Am J Rhinol 2008;22:602-5.
12. Renne R, Brix A, Harkema J, Herbert R, Kittel B, Lewis D, et al. Proliferative and nonproliferative lesions of the rat and mouse respiratory tract. Toxicol Pathol 2009;37:5s-73s.
13. Kuhar HN, Tajudeen BA, Mahdavinia M, Gattuso P, Ghai R, Batra PS. Inflammatory infiltrate and mucosal remodeling in chronic rhinosinusitis with and without polyps: structured histopathologic analysis. Int Forum Allergy Rhinol 2017;7:679-89.
14. Barham HP, Osborn JL, Snidvongs K, Mrad N, Sacks R, Harvey RJ. Remodeling changes

of the upper airway with chronic rhinosinusitis. Int Forum Allergy Rhinol 2015;5:565-72.

15. Snidvongs K, Lam M, Sacks R, Earls P, Kalish L, Phillips PS, et al. Structured histopathology profiling of chronic rhinosinusitis in routine practice. Int Forum Allergy Rhinol 2012;2:376-85.
16. Goyette J, Geczy CL. Inflammation-associated S100 proteins: new mechanisms that regulate function. Amino Acids 2011;41:821-42.
17. Vogl T, Gharibyan AL, Morozova-Roche LA. Pro-inflammatory S100A8 and S100A9 proteins: self-assembly into multifunctional native and amyloid complexes. Int J Mol Sci 2012;13:2893-917.
18. Pruenster M, Vogl T, Roth J, Sperandio M. S100A8/A9: From basic science to clinical application. Pharmacol Ther 2016;167:120-31.
19. Voss A, Bode G, Sopalla C, Benedyk M, Varga G, Böhm M, et al. Expression of S100A8/A9 in HaCaT keratinocytes alters the rate of cell proliferation and differentiation. FEBS Lett 2011;585:440-6.
20. Tieu DD, Peters AT, Carter RG, Suh L, Conley DB, Chandra R, et al. Evidence for diminished levels of epithelial psoriasin and calprotectin in chronic rhinosinusitis. J Allergy Clin Immunol 2010;125:667-75.
21. Richer SL, Truong-Tran AQ, Conley DB, Carter R, Vermylen D, Grammer LC, et al. Epithelial genes in chronic rhinosinusitis with and without nasal polyps. Am J Rhinol 2008;22:228-34.
22. Boruk M, Railwah C, Lora A, Nath S, Wu D, Chow L, et al. Elevated S100A9 expression in chronic rhinosinusitis coincides with elevated MMP production and proliferation in vitro. Sci Rep 2020;10:16350.
23. Van Crombruggen K, Vogl T, Pérez-Novo C, Holtappels G, Bachert C. Differential release and deposition of S100A8/A9 proteins in inflamed upper airway tissue. Eur Respir J 2016;47:264-74.
24. Fokkens WJ, Lund VJ, Hopkins C, Hellings PW, Kern R, Reitsma S, et al. European Position Paper on Rhinosinusitis and Nasal Polyps 2020. Rhinology 2020;58:1-464.
25. Lund VJ, Mackay IS. Staging in rhinosinusitus. Rhinology 1993;31:183-4.
26. Ha JG, Kim J, Nam JS, Park JJ, Cho HJ, Yoon JH, et al. Development of a Korean Culture-Friendly Olfactory Function Test and Optimization of a Diagnostic Cutoff Value.

Clin Exp Otorhinolaryngol 2020;13:274-84.

27. Yoon JH, Moon HJ, Seong JK, Kim CH, Lee JJ, Choi JY, et al. Mucociliary differentiation according to time in human nasal epithelial cell culture. Differentiation 2002;70:77-83.

28. Yoon JH, Hong SS, Hong JP, Lee GY, Park IY. Rate of Synthesis and Degradation of Lysozyme Protein by Retinoic Acid in Normal Human Airway Epithelial Cells. Korean J Otorhinolaryngol-Head Neck Surg 1999;42:981-4.

29. Gao T, Ng CL, Li C, Li YY, Duan C, Shen L, et al. Smoking is an independent association of squamous metaplasia in Chinese nasal polyps. Int Forum Allergy Rhinol 2016;6:66-74.

30. Huang H, Tan KS, Zhou S, Yuan T, Liu J, Ong HH, et al. p63(+)Krt5(+) basal cells are increased in the squamous metaplastic epithelium of patients with radiation-induced chronic Rhinosinusitis. Radiat Oncol 2020;15:222.

31. Gallego O, Belyaeva OV, Porté S, Ruiz FX, Stetsenko AV, Shabrova EV, et al. Comparative functional analysis of human medium-chain dehydrogenases, short-chain dehydrogenases/reductases and aldo-keto reductases with retinoids. Biochem J 2006;399:101-9.

32. Hobbs JA, May R, Tanousis K, McNeill E, Mathies M, Gebhardt C, et al. Myeloid cell function in MRP-14 (S100A9) null mice. Mol Cell Biol 2003;23:2564-76.

33. Hsu K, Passey RJ, Endoh Y, Rahimi F, Youssef P, Yen T, et al. Regulation of S100A8 by glucocorticoids. J Immunol 2005;174:2318-26.

34. Xu K, Yen T, Geczy CL. Il-10 up-regulates macrophage expression of the S100 protein S100A8. J Immunol 2001;166:6358-66.

35. Yen T, Harrison CA, Devery JM, Leong S, Iismaa SE, Yoshimura T, et al. Induction of the S100 chemotactic protein, CP-10, in murine microvascular endothelial cells by proinflammatory stimuli. Blood 1997;90:4812-21.

36. Mørk G, Schjerven H, Mangschau L, Søyland E, Brandtzaeg P. Proinflammatory cytokines upregulate expression of calprotectin (L1 protein, MRP-8/MRP-14) in cultured human keratinocytes. Br J Dermatol 2003;149:484-91.

37. Hu SP, Harrison C, Xu K, Cornish CJ, Geczy CL. Induction of the chemotactic S100 protein, CP-10, in monocyte/macrophages by lipopolysaccharide. Blood

1996;87:3919-28.

38. Pinet K, McLaughlin KA. Mechanisms of physiological tissue remodeling in animals: Manipulating tissue, organ, and organism morphology. Dev Biol 2019;451:134-45.
39. Kim SW, Cheon K, Kim CH, Yoon JH, Hawke DH, Kobayashi R, et al. Proteomics-based identification of proteins secreted in apical surface fluid of squamous metaplastic human tracheobronchial epithelial cells cultured by three-dimensional organotypic air-liquid interface method. Cancer Res 2007;67:6565-73.
40. Donato R, Cannon BR, Sorci G, Riuzzi F, Hsu K, Weber DJ, et al. Functions of S100 proteins. Curr Mol Med 2013;13:24-57.
41. Konieczny P, Xing Y, Sidhu I, Subudhi I, Mansfield KP, Hsieh B, et al. Interleukin-17 governs hypoxic adaptation of injured epithelium. Science 2022;377:eabg9302.
42. Lee SN, Lee DH, Lee MG, Yoon JH. Proprotein convertase 5/6a is associated with bone morphogenetic protein-2-induced squamous cell differentiation. Am J Respir Cell Mol Biol 2015;52:749-61.
43. Hsu K, Champaiboon C, Guenther BD, Sorenson BS, Khammanivong A, Ross KF, et al. ANTI-INFECTIVE PROTECTIVE PROPERTIES OF S100 CALGRANULINS. Antiinflamm Antiallergy Agents Med Chem 2009;8:290-305.
44. Lagasse E, Clerc RG. Cloning and expression of two human genes encoding calcium-binding proteins that are regulated during myeloid differentiation. Mol Cell Biol 1988;8:2402-10.
45. Hessian PA, Edgeworth J, Hogg N. MRP-8 and MRP-14, two abundant Ca(2+)-binding proteins of neutrophils and monocytes. J Leukoc Biol 1993;53:197-204.
46. Voganatsi A, Panyutich A, Miyasaki KT, Murthy RK. Mechanism of extracellular release of human neutrophil calprotectin complex. J Leukoc Biol 2001;70:130-4.
47. Lemarchand P, Vaglio M, Mauël J, Markert M. Translocation of a small cytosolic calcium-binding protein (MRP-8) to plasma membrane correlates with human neutrophil activation. J Biol Chem 1992;267:19379-82.
48. Clark HL, Jhingran A, Sun Y, Vareechon C, de Jesus Carrion S, Skaar EP, et al. Zinc and Manganese Chelation by Neutrophil S100A8/A9 (Calprotectin) Limits Extracellular Aspergillus fumigatus Hyphal Growth and Corneal Infection. J Immunol 2016;196:336-44.

49. Damo SM, Kehl-Fie TE, Sugitani N, Holt ME, Rathi S, Murphy WJ, et al. Molecular basis for manganese sequestration by calprotectin and roles in the innate immune response to invading bacterial pathogens. Proc Natl Acad Sci U S A 2013;110:3841-6.
50. Nakashige TG, Zhang B, Krebs C, Nolan EM. Human calprotectin is an iron-sequestering host-defense protein. Nat Chem Biol 2015;11:765-71.
51. Urban CF, Ermert D, Schmid M, Abu-Abed U, Goosmann C, Nacken W, et al. Neutrophil extracellular traps contain calprotectin, a cytosolic protein complex involved in host defense against Candida albicans. PLoS Pathog 2009;5:e1000639.
52. Kato A, Peters AT, Stevens WW, Schleimer RP, Tan BK, Kern RC. Endotypes of chronic rhinosinusitis: Relationships to disease phenotypes, pathogenesis, clinical findings, and treatment approaches. Allergy 2022;77:812-26.
53. Candar T, Baklaci D, Kuzucu I, Kayabasi S. A proinflammatory marker in chronic rhinosinusitis: serum calprotectin. Acta Biochim Pol 2020;67:367-71.
54. Takabayashi T, Schleimer RP. Formation of nasal polyps: The roles of innate type 2 inflammation and deposition of fibrin. J Allergy Clin Immunol 2020;145:740-50.
55. Ryu G, Kim DW. Th2 inflammatory responses in the development of nasal polyps and chronic rhinosinusitis. Curr Opin Allergy Clin Immunol 2020;20:1-8.
56. Williams TL, Rada B, Tandon E, Gestal MC. "NETs and EETs, a Whole Web of Mess". Microorganisms 2020;8.
57. Ueki S, Tokunaga T, Fujieda S, Honda K, Hirokawa M, Spencer LA, et al. Eosinophil ETosis and DNA Traps: a New Look at Eosinophilic Inflammation. Curr Allergy Asthma Rep 2016;16:54.
58. Curran CS, Bertics PJ. Human eosinophils express RAGE, produce RAGE ligands, exhibit PKC-delta phosphorylation and enhanced viability in response to the RAGE ligand, S100B. Int Immunol 2011;23:713-28.
59. Wilkerson EM, Johansson MW, Hebert AS, Westphall MS, Mathur SK, Jarjour NN, et al. The Peripheral Blood Eosinophil Proteome. J Proteome Res 2016;15:1524-33.
60. Park SC, Kim SI, Hwang CS, Cho HJ, Yoon JH, Kim CH. Multiple airborne allergen-induced eosinophilic chronic rhinosinusitis murine model. Eur Arch Otorhinolaryngol 2019;276:2273-82.
61. Tokunaga T, Sakashita M, Haruna T, Asaka D, Takeno S, Ikeda H, et al. Novel scoring

system and algorithm for classifying chronic rhinosinusitis: the JESREC Study. Allergy 2015;70:995-1003.

62. Dworski R, Simon HU, Hoskins A, Yousefi S. Eosinophil and neutrophil extracellular DNA traps in human allergic asthmatic airways. J Allergy Clin Immunol 2011;127:1260-6.

63. Fukuchi M, Miyabe Y, Furutani C, Saga T, Moritoki Y, Yamada T, et al. How to detect eosinophil ETosis (EETosis) and extracellular traps. Allergol Int 2021;70:19-29.

64. Yousefi S, Simon D, Stojkov D, Karsonova A, Karaulov A, Simon H-U. In vivo evidence for extracellular DNA trap formation. Cell Death & Disease 2020;11:300.

65. Ferrero-Miliani L, Nielsen OH, Andersen PS, Girardin SE. Chronic inflammation: importance of NOD2 and NALP3 in interleukin-1beta generation. Clin Exp Immunol 2007;147:227-35.

66. Kato T, Kouzaki H, Matsumoto K, Hosoi J, Shimizu T. The effect of calprotectin on TSLP and IL-25 production from airway epithelial cells. Allergol Int 2017;66:281-9.

67. Sipponen T, Kolho KL. Fecal calprotectin in diagnosis and clinical assessment of inflammatory bowel disease. Scand J Gastroenterol 2015;50:74-80.

68. García-Arias M, Pascual-Salcedo D, Ramiro S, Ueberschlag ME, Jermann TM, Cara C, et al. Calprotectin in rheumatoid arthritis : association with disease activity in a cross-sectional and a longitudinal cohort. Mol Diagn Ther 2013;17:49-56.

69. Hansson C, Eriksson C, Alenius GM. S-calprotectin (S100A8/S100A9): a potential marker of inflammation in patients with psoriatic arthritis. J Immunol Res 2014;2014:696415.

70. Lee YG, Hong J, Lee PH, Lee J, Park SW, Kim D, et al. Serum Calprotectin Is a Potential Marker in Patients with Asthma. J Korean Med Sci 2020;35:e362.

71. Quoc QL, Choi Y, Thi Bich TC, Yang E-M, Shin YS, Park H-S. S100A9 in adult asthmatic patients: a biomarker for neutrophilic asthma. Experimental & Molecular Medicine 2021;53:1170-9.

72. Mahler M, Meroni PL, Infantino M, Buhler KA, Fritzler MJ. Circulating Calprotectin as a Biomarker of COVID-19 Severity. Expert Rev Clin Immunol 2021;17:431-43.

73. Tomassen P, Vandeplas G, Van Zele T, Cardell LO, Arebro J, Olze H, et al. Inflammatory endotypes of chronic rhinosinusitis based on cluster analysis of biomarkers. J Allergy

Clin Immunol 2016;137:1449-56.e4.

74. Delemarre T, Bochner BS, Simon HU, Bachert C. Rethinking neutrophils and eosinophils in chronic rhinosinusitis. J Allergy Clin Immunol 2021; doi:10.1016/j.jaci.2021.03.024.

75. Delemarre T, Holtappels G, De Ruyck N, Zhang N, Nauwynck H, Bachert C, et al. A substantial neutrophilic inflammation as regular part of severe type 2 chronic rhinosinusitis with nasal polyps. J Allergy Clin Immunol 2021;147:179-88.e2.

76. Poposki JA, Klingler AI, Stevens WW, Suh LA, Tan BK, Peters AT, et al. Elevation of activated neutrophils in chronic rhinosinusitis with nasal polyps. J Allergy Clin Immunol 2022;149:1666-74.

77. Wang S, Song R, Wang Z, Jing Z, Wang S, Ma J. S100A8/A9 in Inflammation. Front Immunol 2018;9:1298.

78. Wang H, Pan L, Liu Z. Neutrophils as a Protagonist and Target in Chronic Rhinosinusitis. Clin Exp Otorhinolaryngol 2019;12:337-47.

79. Ahn SH, Lee EJ, Ha JG, Hwang CS, Yoon JH, Kim CH, et al. Comparison of olfactory and taste functions between eosinophilic and non-eosinophilic chronic rhinosinusitis. Auris Nasus Larynx 2020;47:820-7.

80. Hwang CS, Park SC, Cho HJ, Park DJ, Yoon JH, Kim CH. Eosinophil extracellular trap formation is closely associated with disease severity in chronic rhinosinusitis regardless of nasal polyp status. Sci Rep 2019;9:8061.

ABSTRACT (IN KOREAN)

S100A8/S100A9 (calprotectin)이 사람 호흡기 점막 상피에 미치는 영향과 조절 기전

<지도교수 김창훈>

연세대학교 대학원 의학과

안상현

염증은 외부 자극에 대한 숙주의 방어 기제로 상기도의 첫 번째 장벽인 비강 점막 상피세포와 점막 하층에 분포하는 염증세포에 의한 복합적인 면역반응으로 인해 발생한다. 비강과 부비동에 발생하는 염증성 질환인 만성 비부비동염은 점막 상피세포와 다수의 염증 관련 단백질, 그리고 다양한 면역세포가 관여하고 있으며 이들과 관련한 다양한 병태생리학적 면역 기전이 제시되어 있다. 특히, S100A8과 S100A9의 이종이량체 복합체인 calprotectin (칼프로텍틴)은 손상 관련 분자 패턴으로써 비강 점막 상피 세포와 염증 세포에서 다양한 기능을 수행하며 S100A8과 S100A9는 강력한 전염증 효과가 있는 것으로 알려져 있다. 하지만 이 단백질들이 비강 점막 상피세포에 미치는 영향과 만성 비부비동염의 발병 기전에 대한 연구는 아직까지 드물다. 따라서 본 연구에서는 S100A8, S100A9 및 칼프로텍틴이 비강 점막 상피세포와 비강의 염증성 질환인 만성 비부비동염에 미치는 영향과 조절 기전을 조사하였다.

1장에서는 S100A8과 S100A9이 비강 점막 상피세포에서 증가되는 조건과 그 역할을 조사하였다. S100A8과 S100A9는 비강 점막 상피세포에서 TNF-α 및

IL-1β와 같은 전염증성 사이토카인을 처리했을 때 증가했고, IL-4 및 IL-13과 같은 항염증성 사이토카인에 의해 억제되었다. 또한, 만성 비부비동염 환자의 조직을 가지고 면역조직화학염색을 시행하고 분석하였다. 그 결과는 S100A8과 S100A9이 정상 상피층이 아닌 편평 상피층에서 과발현되었다. 이를 통해 S100A8과 S100A9이 비강 점막 상피세포의 편평 상피 화생에 영향을 미치는지 알아보기 위한 실험을 진행하였다. 배양된 비강 점막 상피세포에 재조합 S100A8, S100A9, 칼프로텍틴을 각각 처리한 후 조직 리모델링 표지자인 MMP9와 편평 상피 화생의 표지자인 Involucrin의 발현을 확인하였다. S100A8과 S100A9이 편평 상피 화생에 영향을 주는 최적의 실험 조건을 확인하였고 bulk RNA 시퀀싱 분석을 통해 S100A8, S100A9, 칼프로텍틴이 비강 점막 상피세포에 미치는 영향을 확인하였다. 이 실험을 통해 S100A8과 S100A9, 그리고 칼프로텍틴이 비강 점막 상피세포에 미치는 공통점과 차이점을 확인할 수 있었다. 특히, S100A9는 비강 점막 상피세포 분화에 중요한 레티노산 대사에 관여한다는 것을 확인하였고, 편평 상피 화생과 조직 리모델링에 관련이 있는 것을 확인하였다.

2장에서는 만성 비부비동염의 병태생리학에서 중요한 염증세포로 알려진 호산구와 그와 관련한 호산구 세포외 트랩에 대하여 항균 펩타이드로 알려진 칼프로텍틴의 관련성을 조사하였다. 기존의 문헌들에 따르면 칼프로텍틴은 주로 호중구에서 발현되며, 선천적 염증 반응에 중요한 호중구 세포외 트랩에 관여하는 것으로 알려져 있었다. 하지만 비용종을 동반한 만성 비부비동염은 호산구가 질병 발달에 중요한 제2형 염증 질환으로 알려져 있어 칼프로텍틴과 호중구만을 설명하기에는 불충분하였다. 따라서 본 연구의 목적은 호산구에서 칼프로텍틴의 발현을 확인하고 칼프로텍틴과 호산구 세포외 트랩의 관계를 조사하였다. 이 가설을 증명하기 위해 호산구성 만성 비부비동염 마우스 모델과 만성 비부비동염 환자의 조직을 사용하여 각각 호산구 및 호중구에 특이적인

표지자인 major basic protein (MBP)와 myeloperoxidase (MPO), 그리고 칼프로텍틴 항체를 가지고 동시에 삼중 면역 형광 염색을 진행하였다. 칼프로텍틴 양성 세포는 MPO 양성 세포와 일치할 뿐만 아니라 MBP에 양성을 나타내는 세포도 일치하는 소견을 보였다. 이를 통해 칼프로텍틴이 호중구와 호산구에서 각각 발현되는 것을 확인할 수 있었다. 또한, 칼프로텍틴은 호중구 세포외 트랩뿐만 아니라 호산구 세포외 트랩에서도 발현되는 것을 확인하였다. 이 결과를 통해 조직 내 칼프로텍틴 양성 세포가 많을 수록 조직 및 혈액의 호산구가 비례하게 증가하는 임상적인 의미를 발견할 수 있었다. 뿐만 아니라 칼프로텍틴을 발현하는 염증세포는 후각장애, 만성 비부비동염의 중증도를 나타내는 Lund-Mackay CT 점수, JECREC 점수와 상관관계를 보였다. 결국, 이 연구를 통해 만성 비부비동염의 조직에서 칼프로텍틴의 발현이 만성 비부비동염의 중증도를 나타내는 바이오마커가 될 수 있음을 입증하였다.

이 두 연구를 요약하면, 비강 점막 상피세포에서 염증에 의해 증가된 S100A8과 S1000A9는 레티노이드 대사의 조절에 관여하고 편평 상피 화생과 같은 조직 리모델링을 유도하였다. 또한, 이들의 복합체인 칼프로텍틴은 항균 펩타이드로써 호중구와 호산구에서 각각 분비되며 호산구 세포외 트랩에서도 관여하기 때문에 비용종을 동반한 만성 비부비동염의 선천 면역 반응에 중요한 역할을 하였다. 결론적으로 본 연구를 통해 비강 상피 점막세포와 염증세포에서 발현되는 S100A8, S100A9, 칼프로텍틴은 만성 비부비동염 환자의 질병 중증도를 반영하는 중요한 생체 지표가 될 수 있음을 확인하였다.

핵심되는 말: S100A8, S100A9, 칼프로텍틴, 코 점막, 조직 리모델링, 부비동염, 비용종, 항균 펩타이드, 호산구, 세포외 트랩

PUBLICATION LIST

Oh JT, Shin KH, Paik SY, **Ahn SH**. A case of high-grade B cell lymphoma, not otherwise specified originating from inferior turbinate. Korean J Otorhinolaryngol-Head Neck Surg 2022;65:834-8

Nam JS, **Ahn SH**, Ha JG, Park JJ, Noh HE, Yoon JH, et al. Differential Correlations among Allergy Tests According to Indoor Allergens in Allergic Rhinitis. Ann Otol Rhinol Laryngol 2022;131:71-7.

Ahn SH, Jeong Y, Shin GC, Yoon JH, Kim CH, Cho HJ. Outcomes of multilevel upper airway surgery, including tongue base resection, in patients with torus mandibularis. J Craniomaxillofac Surg 2021;49:682-7.

Kang JC, Shin KH, Kwon KW, **Ahn SH**. A Case of Choanal Polyp Originated from the Inferior Turbinate. Korean J Otorhinolaryngol-Head Neck Surg 2020;63:611-4.

Kang JC, Shin KH, Han EM, **Ahn SH**. A Case of Nasopalatine Duct Cyst with Cholesterol Granuloma in Maxillary Sinus. Korean J Otorhinolaryngol-Head Neck Surg 2020;63:528-32.

Ahn SH, Lee EJ, Ha JG, Hwang CS, Yoon JH, Kim CH, et al. Comparison of olfactory and taste functions between eosinophilic and non-eosinophilic chronic rhinosinusitis. Auris Nasus Larynx 2020;47:820-7.

Ahn SH, Lee EJ, Hong MP, Shin GC, Kim KS. Comparison of the clinical characteristics of bilateral and unilateral fungal balls in Korea. Eur Arch Otorhinolaryngol 2019;276:1975-80.

Ahn SH, Ha JG, Kim JW, Lee YW, Yoon JH, Kim CH, et al. Torus mandibularis affects the severity and position-dependent sleep apnoea in non-obese patients. Clin Otolaryngol 2019;44:279-85.

Ahn SH, Lee EJ, Kim JW, Baek KH, Cho HJ, Yoon JH, et al. Better surgical outcome by image-guided navigation system in endoscopic removal of sinonasal inverted papilloma. J Craniomaxillofac Surg 2018;46:937-41.

Ahn SH, Kim J, Min HJ, Chung HJ, Hong JM, Lee JG, et al. Tongue Volume Influences Lowest Oxygen Saturation but Not Apnea-Hypopnea Index in Obstructive Sleep Apnea. PLoS One 2015;10:e0135796.

Ahn SH, Lee YJ, Kim CH, Chang JH. Angiomyolipoma of the Nasal Cavity Resected with Preoperative Angio-Embolization. Korean J Otorhinolaryngol-Head Neck Surg 2013;56:528-31.

Ha JG, Min HJ, **Ahn SH**, Kim CH, Yoon JH, Lee JG, et al. The dimension of hyoid bone is independently associated with the severity of obstructive sleep apnea. PLoS One 2013;8:e81590.

Kim K, Kim MJ, **Ahn SH**, Bae SY, Kim WS, Yoon JH. Frontal sinus lymphoma presenting as progressive multiple cranial nerve palsy. Yonsei Med J 2011;52:1044-7.

In Submission

Ahn SH, Shin, KH, Oh JT, Park SC, Rha MS, Kim SI, et al. Calprotectin in chronic rhinosinusitis eosinophil extracellular traps